

## Electronic Supplementary Information

### Fluorescence Enhancement of Quinolines by Protonation

Essi Tervola,<sup>a</sup> Khai-Nghi Truong,<sup>a</sup> Jas S. Ward,<sup>a</sup> Arri Priimagi,<sup>b</sup> Kari Rissanen<sup>\*a</sup>

a. University of Jyväskylä, Department of Chemistry, P.O. BOX 35, Surfontie 9B, 40014 Jyväskylä, Finland. E-mail: kari.t.rissanen@jyu.fi  
b. Smart Photonic Materials, Faculty of Engineering and Natural Sciences, Tampere University, P.O. BOX 541, FI-33101 Tampere, Finland.

### Contents

#### 1. Experimental Section

#### 2. UV-Vis, QY, Binding Constants

#### 3. NMR

#### 4. X-Ray Crystallography

#### 5. Theoretical Methods

#### 6. References

## 1. Experimental Section

### Instrumentation and Chemicals

Quinoline derivatives were acquired commercially (acridine Sigma-Aldrich 97%, isoquinoline Koch-Light Laboratories Ltd. pure, and benzo[*h*]quinoline Sigma-Aldrich 97%) and used without further purification. Absorption spectra were collected using Varian Cary 100, 300 Series II Series UV-Visible Spectrophotometer and fluorescence spectra were collected using Varian Cary Eclipse Fluorescence Spectrophotometer. The measurements were taken in a 1 cm quartz cuvette and the excitation and the emission bandpasses were set to 2.5 nm and 2.5 nm, respectively. All the measurements were performed in room temperature. <sup>1</sup>H Nuclear magnetic resonance was measured using Bruker 300 Avance instrument at 303 K. All the NMR samples were measured in CDCl<sub>3</sub> and spectra were calibrated using 7.26 ppm as a reference peak for the chloroform solvent signal.

## 2. UV-Vis, QY, Binding Constants

The absorption and fluorescence of isoquinoline, acridine, and benzo[*h*]quinoline (Figures S1-S6) were measured in dichloromethane and titrated with six different acids, trifluoroacetic acid (TFA), trichloroacetic acid (TCA), benzenesulfonic acid (BSA), dichloroacetic acid (DCA), dibromoacetic acid (DBA), and chloroacetic acid (CA). The measured data was used to determine the effects of protonation on integrated relative intensity (Figure S7) and fluorescence quantum yield (Figure S8). The integrated relative intensities were determined in respect to the natural fluorescence of compound using that as a zero point. The fluorescence quantum yields were determined from Equation 1<sup>1</sup>

$$\Phi = \Phi_{ref} \frac{\eta^2}{\eta_{ref}^2} \frac{I}{A} \frac{A_{ref}}{I_{ref}} \quad (1)$$

where  $\Phi$  is quantum yield,  $\eta$  is the solvent refractive index,  $I$  is integrated fluorescence intensity and  $A$  is the absorbance of the compound at the excitation wavelength.

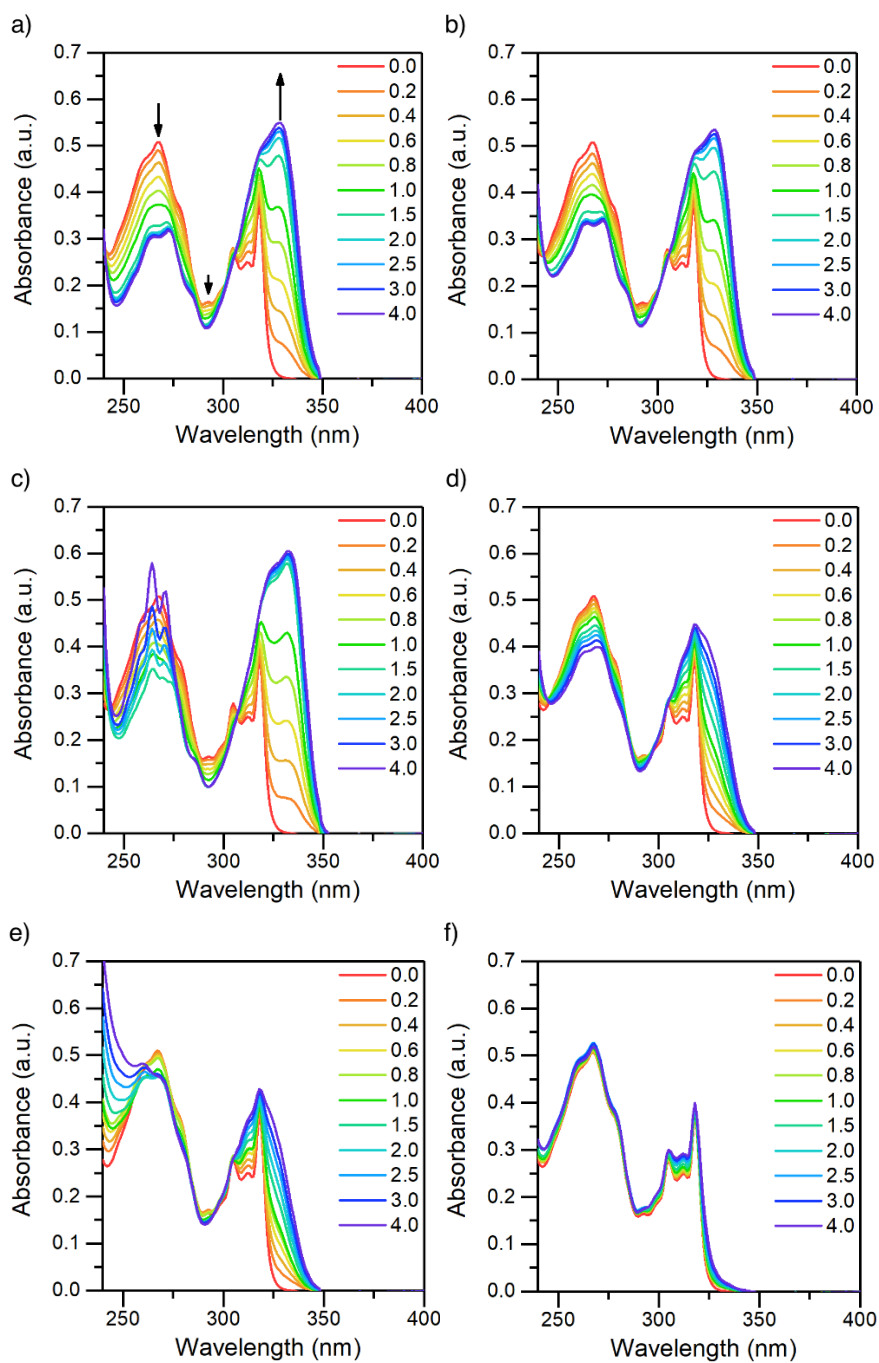


**Figure S1.** Absorption spectra of isoquinoline while titrating with a) TFA b) TCA c) BSA d) DCA e) DBA or f) CA from 0.0 to 4.0 equivalence of the acid (in DCM,  $10^{-4}$  M).



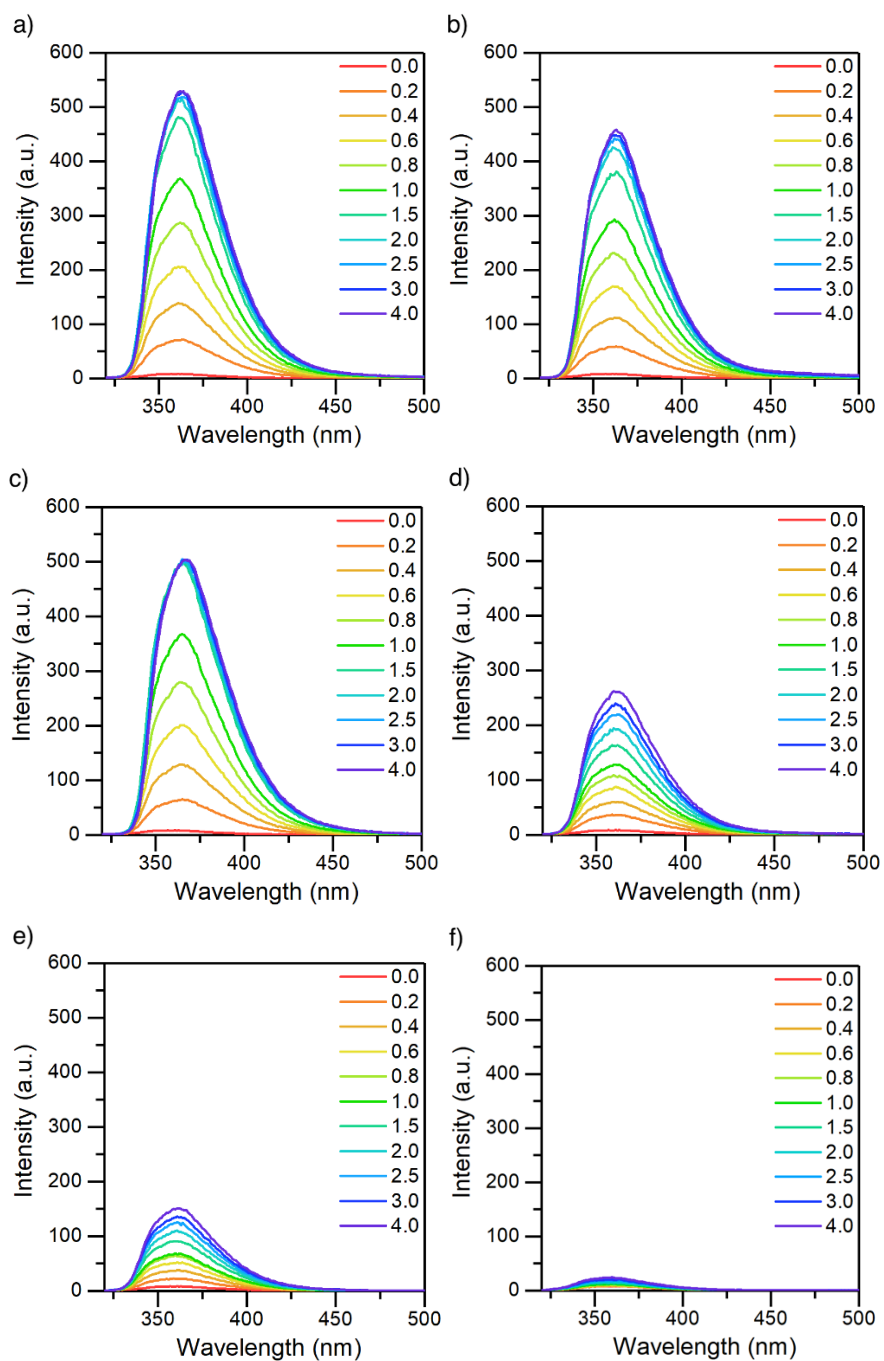


**Figure S2.** The fluorescence spectra of isoquinoline while titrating with a) TFA b) TCA c) BSA d) DCA e) DBA or f) CA from 0.0 to 4.0 equivalence of the acid (in DCM,  $10^{-4}$  M,  $\lambda_{ex} = 310$  nm).

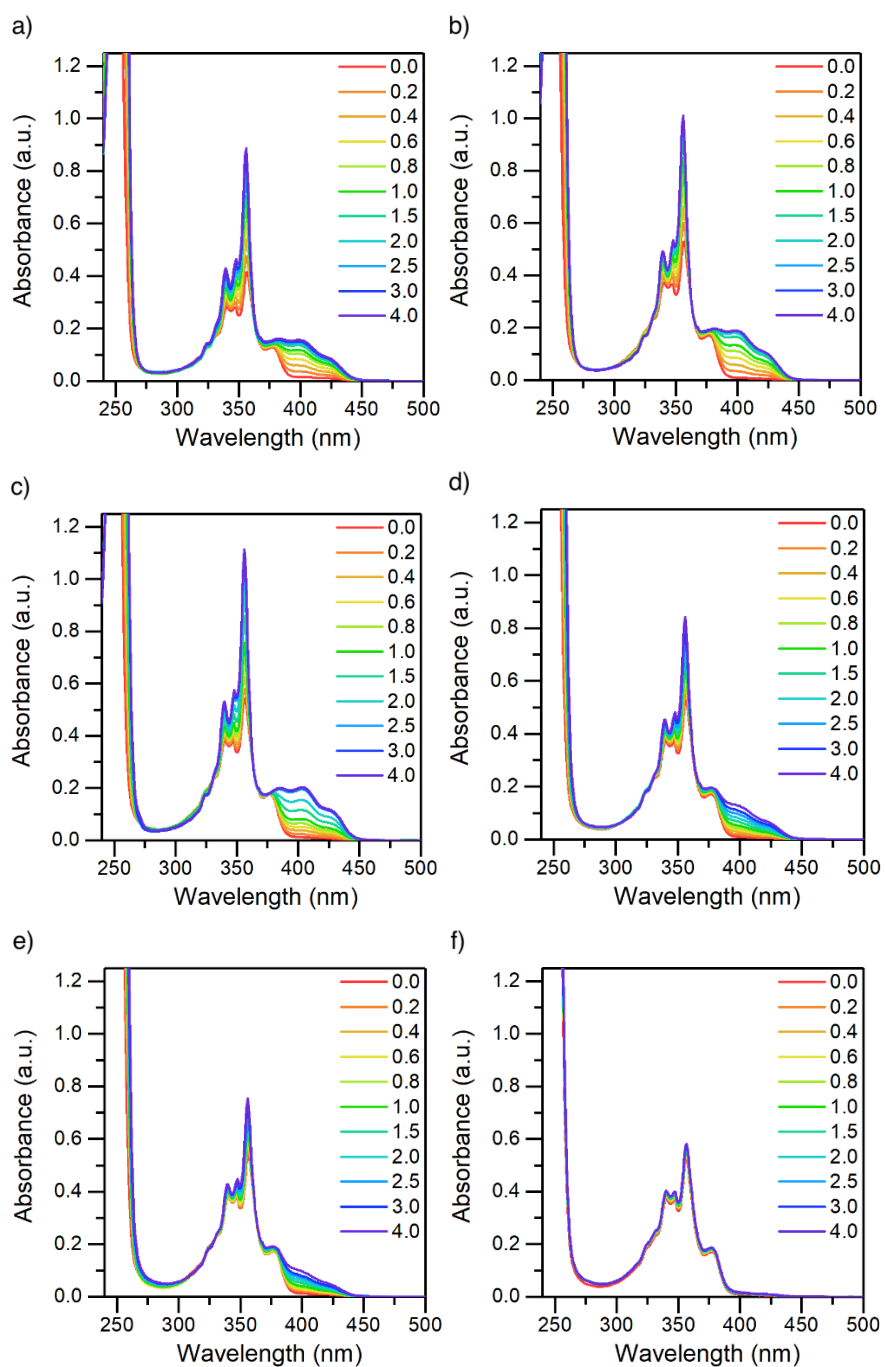


**Figure S3.** Absorption spectra of acridine while titrating with a) TFA b) TCA c) BSA d) DCA e) DBA or f) CA from 0.0 to 4.0 equivalence of the acid (in DCM,  $5 \times 10^{-5}$  M).

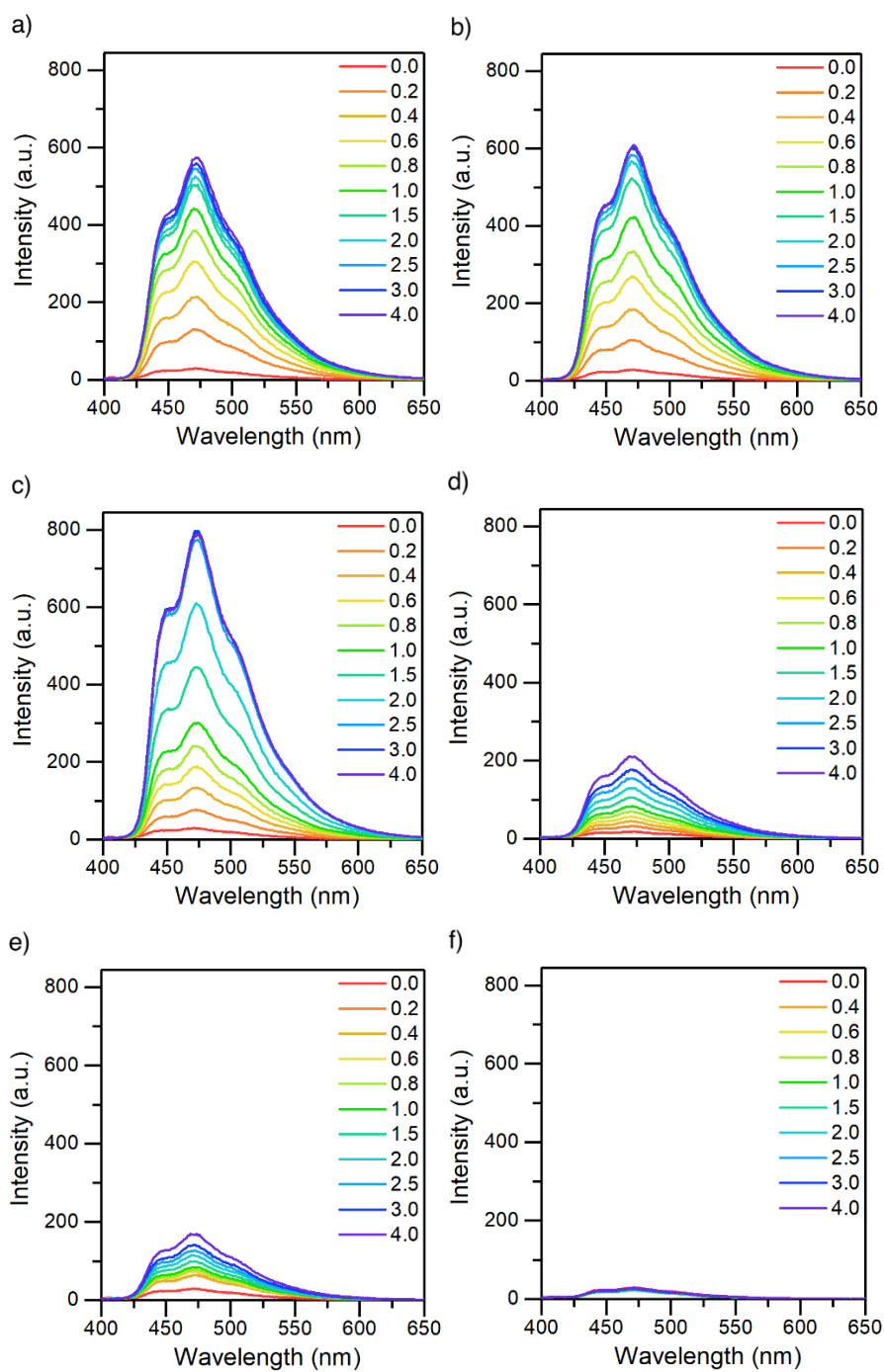


**Figure S4.** The fluorescence spectra of acridine while titrating with a) TFA b) TCA c) BSA d) DCA e) DBA or f) CA from 0.0 to 4.0 equivalence of the acid (in DCM,  $5 \times 10^{-5}$  M,  $\lambda_{ex} = 355$  nm).

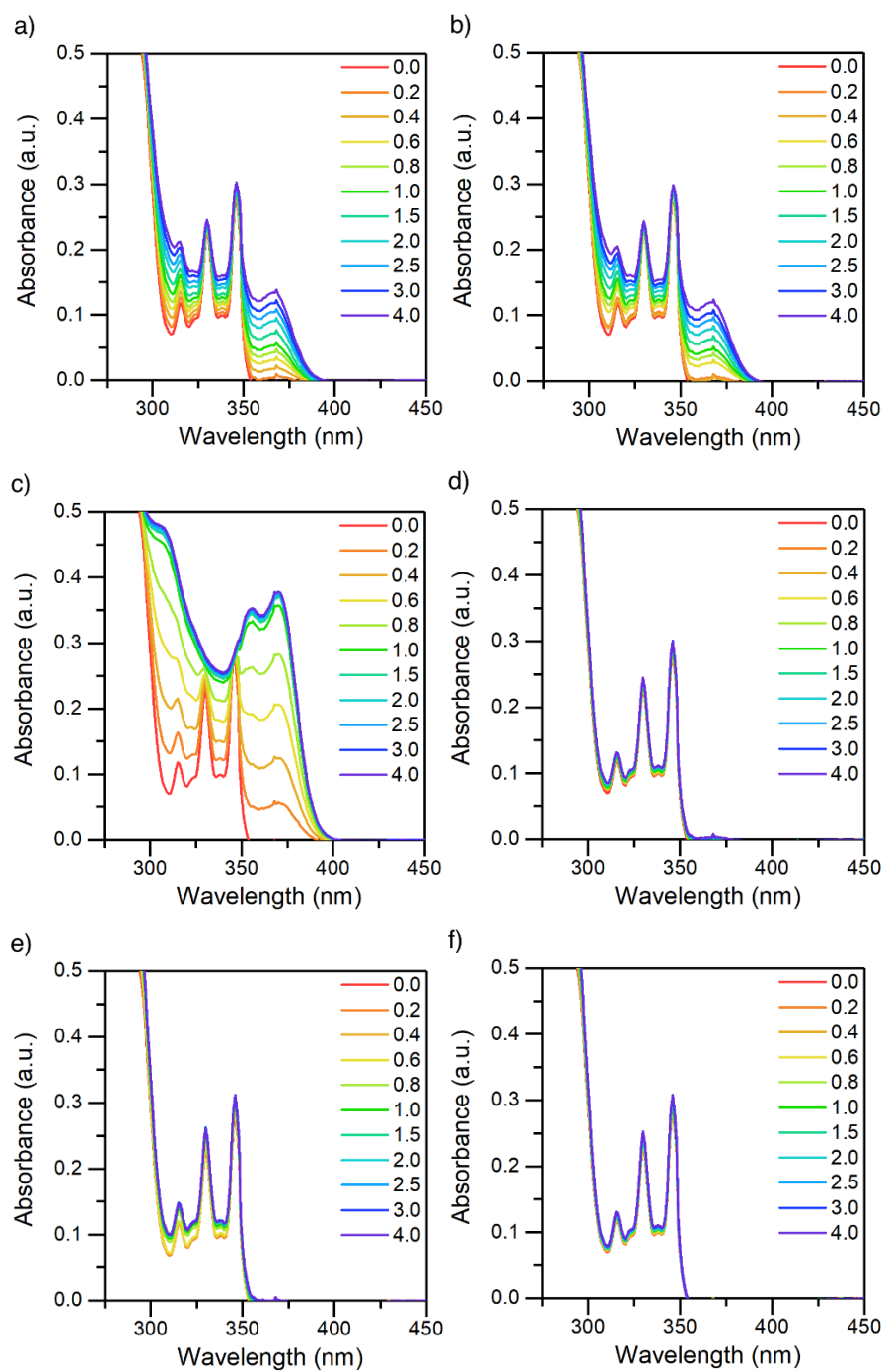


**Figure S5.** Absorption spectra of benzo[*h*]quinoline while titrating with a) TFA b) TCA c) BSA d) DCA e) DBA or f) CA from 0.0 to 4.0 equivalence of the acid (in DCM,  $10^{-4}$  M).

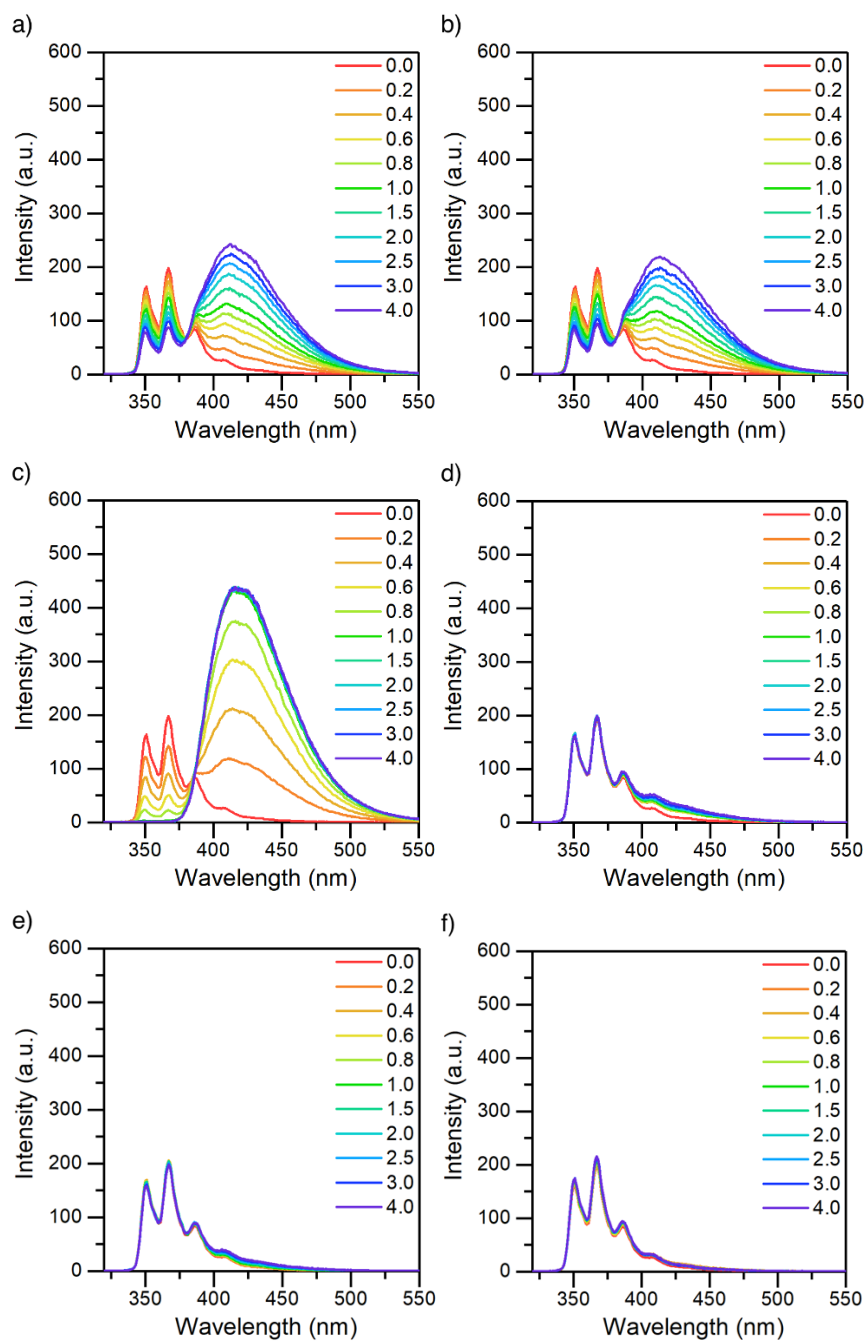


**Figure S6.** The fluorescence spectra of benzo[h]quinoline while titrating with a) TFA b) TCA c) BSA d) DCA e) DBA or f) CA from 0.0 to 4.0 equivalence of the acid (in DCM,  $10^{-4}$  M,  $\lambda_{ex} = 310$  nm).

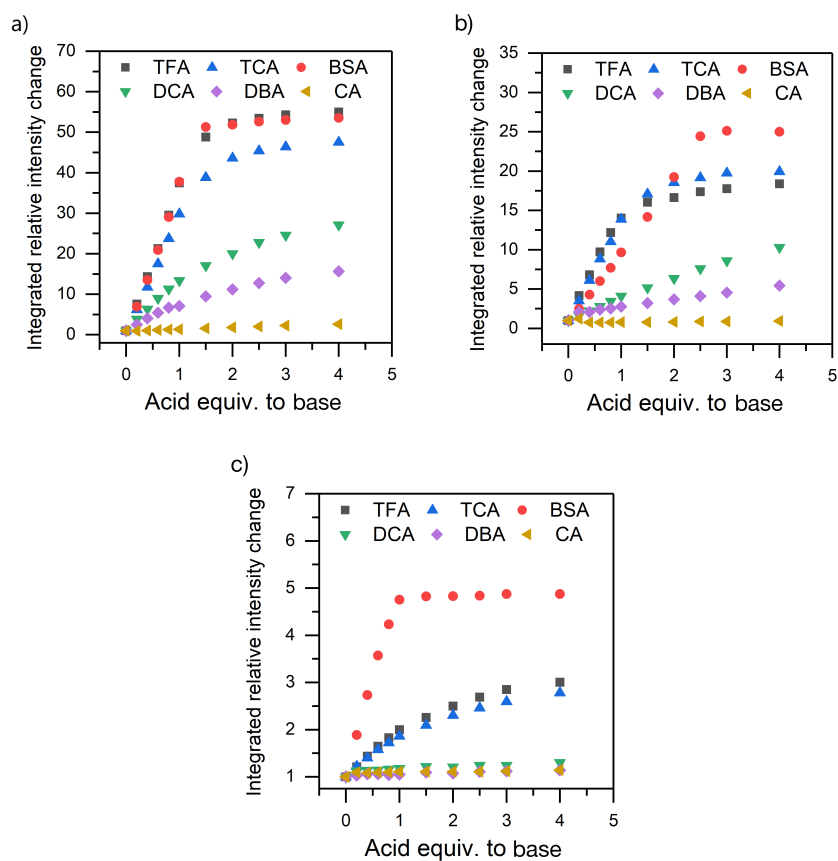


**Figure S7.** Integrated relative fluorescence intensities of a) isoquinoline b) acridine and c) benzo[h]quinoline upon titration with various acids.

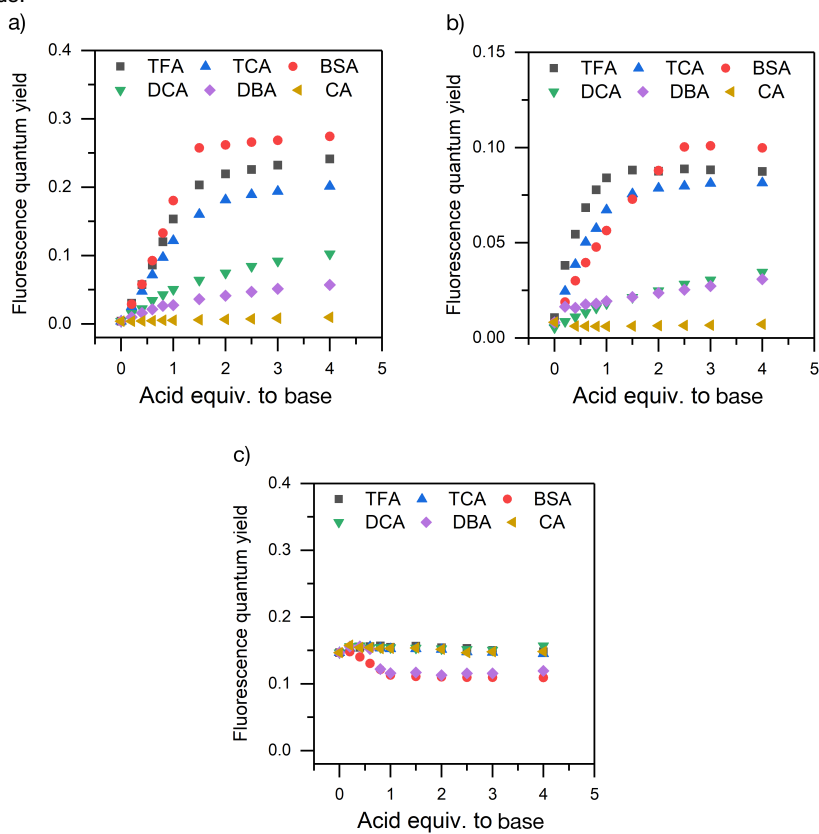


**Figure S8.** Fluorescence quantum yields of a) isoquinoline b) acridine and c) benzo[h]quinoline in DCM.

## 2.1 Determination of the binding constants

Binding constants were determined for isoquinoline in the ground state from absorption spectra while titrating with acid. Absorption bands were assigned for the neutral and cationic species and the changes in the absorption spectra were used to determine the ratio of  $c(\text{bound})$  and  $c(\text{unbound})$ . Binding constants for the ground state are determined using Eq. 1 [2]

$$\frac{c(\text{bound})}{c(\text{unbound})} = K_a[Q] \quad (1)$$

where  $K_a$  is the binding constant for the protonation of the base and  $[Q]$  is the concentration of the added acid.

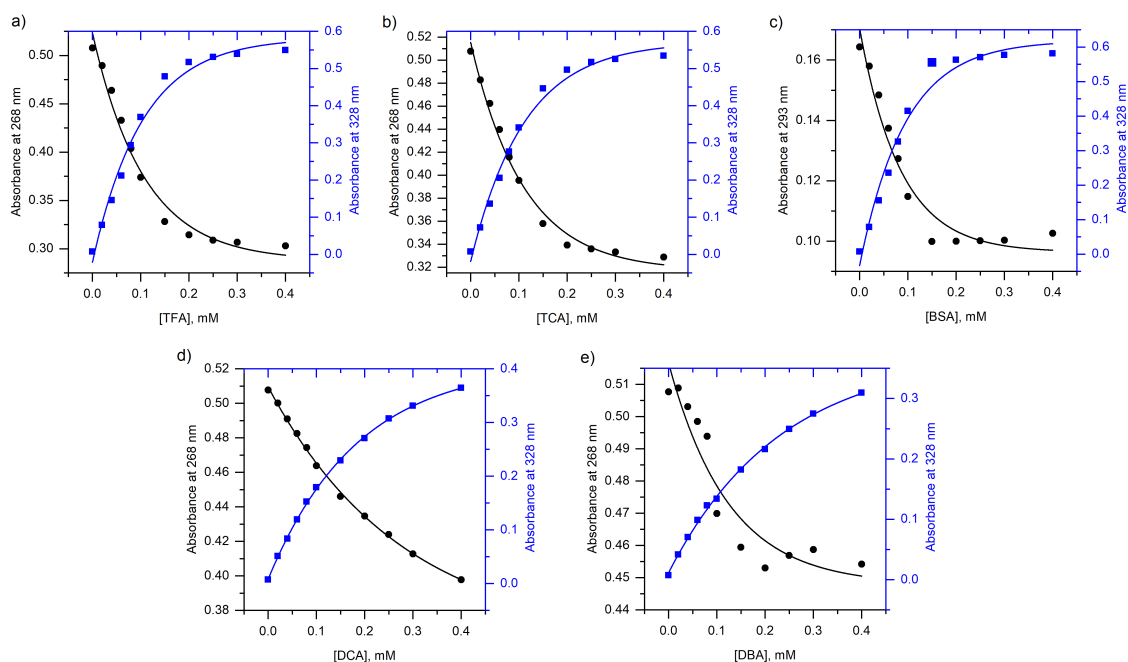


**Figure S9.** The absorbance of isoquinoline (10<sup>-4</sup> M in DCM) at 268/328 nm while titrating with a) TFA b) TCA c) BSA d) DCA e) DBA.

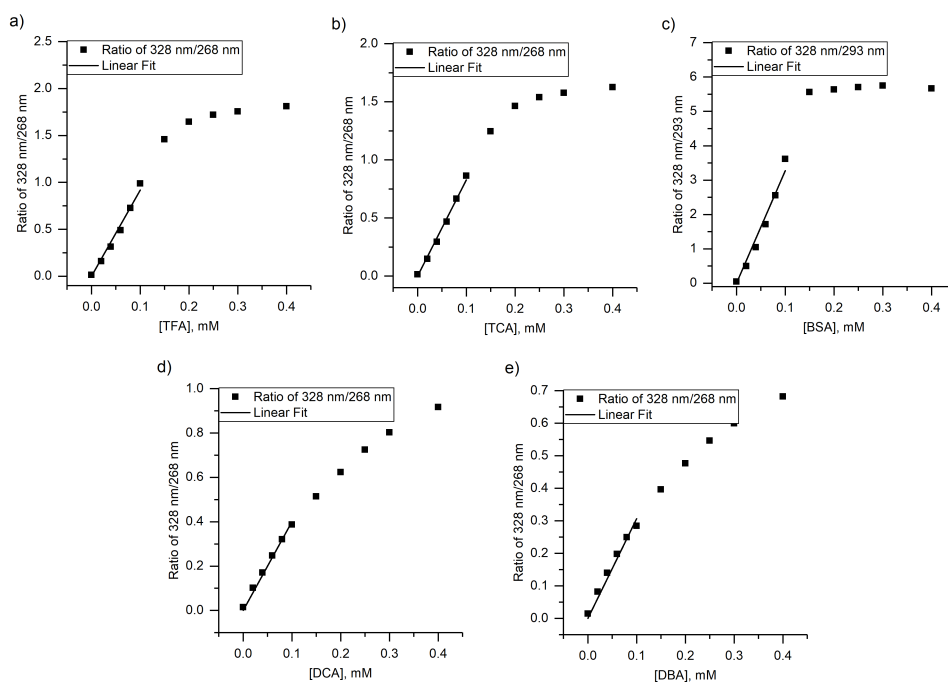


**Figure S10.** The ratio of isoquinolines absorbance at 328/268 nm and its linear fit determined prior to saturation.

### 3. NMR Studies

$^1\text{H}$  NMR was used to further study the effect of protonation on N-heterocycles.  $^1\text{H}$  NMR for all the compounds with all the acids were measured in 1:1 ratio in  $\text{CDCl}_3$  (Figures S9-S11).  $^1\text{H}$  NMR was also attempted to use for the determination of binding constant for the acid-base interactions (Figure S12), but the method was determined unsuitable for this case due to high binding affinities and the uncertainty in their determination.

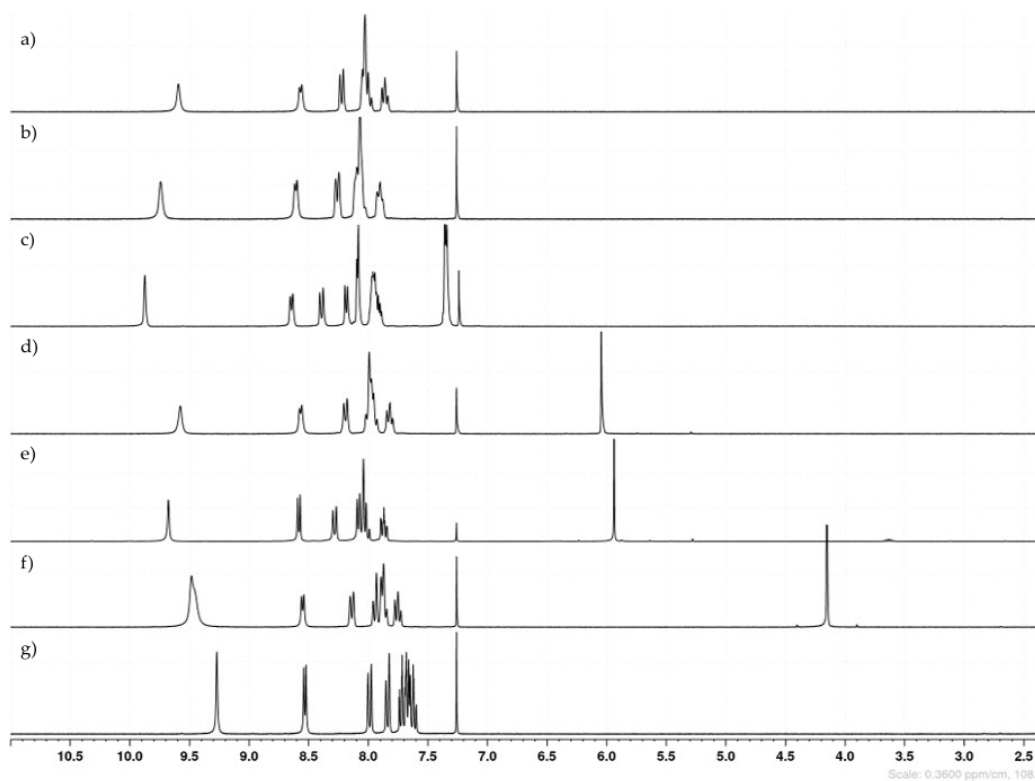


**Figure S11.**  $^1\text{H}$  NMR spectra of isoquinoline with 1:1 ratio of a) TFA b) TCA c) BSA d) DCA e) DBA f) CA and g) on its own ( $\text{CDCl}_3$ , 303 K, 300 MHz, 30 mM).



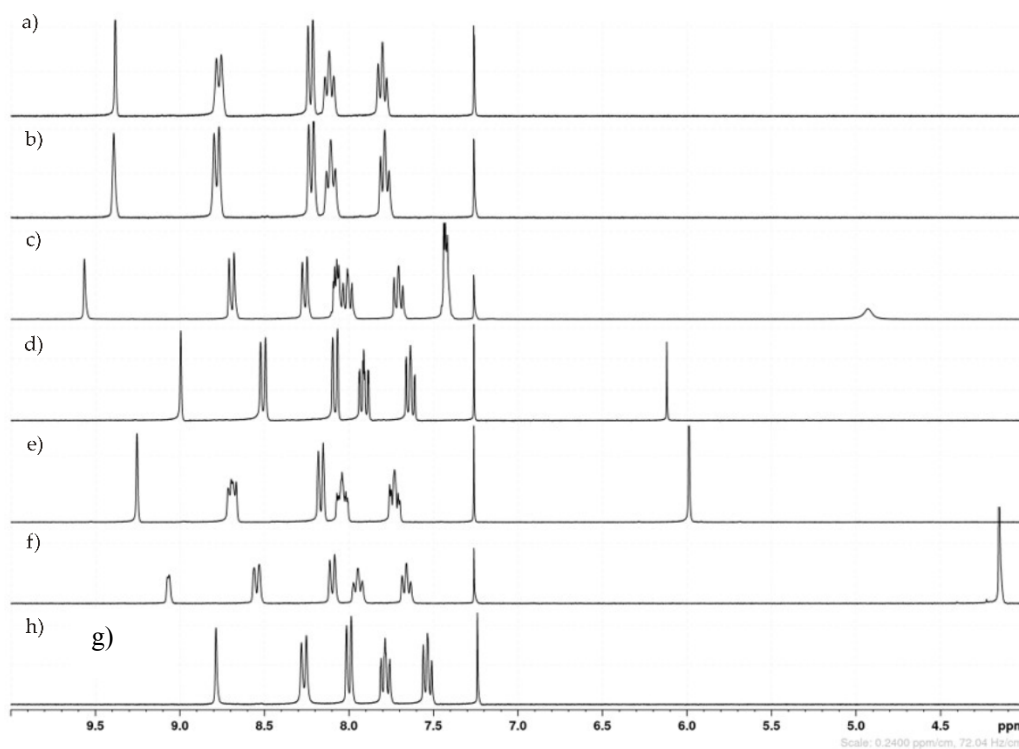


**Figure S12.**  $^1\text{H}$  NMR spectra of acridine with 1:1 ratio of a) TFA b) TCA c) BSA d) DCA e) DBA f) CA and g) on its own ( $\text{CDCl}_3$ , 303 K, 300 MHz, 30 mM).

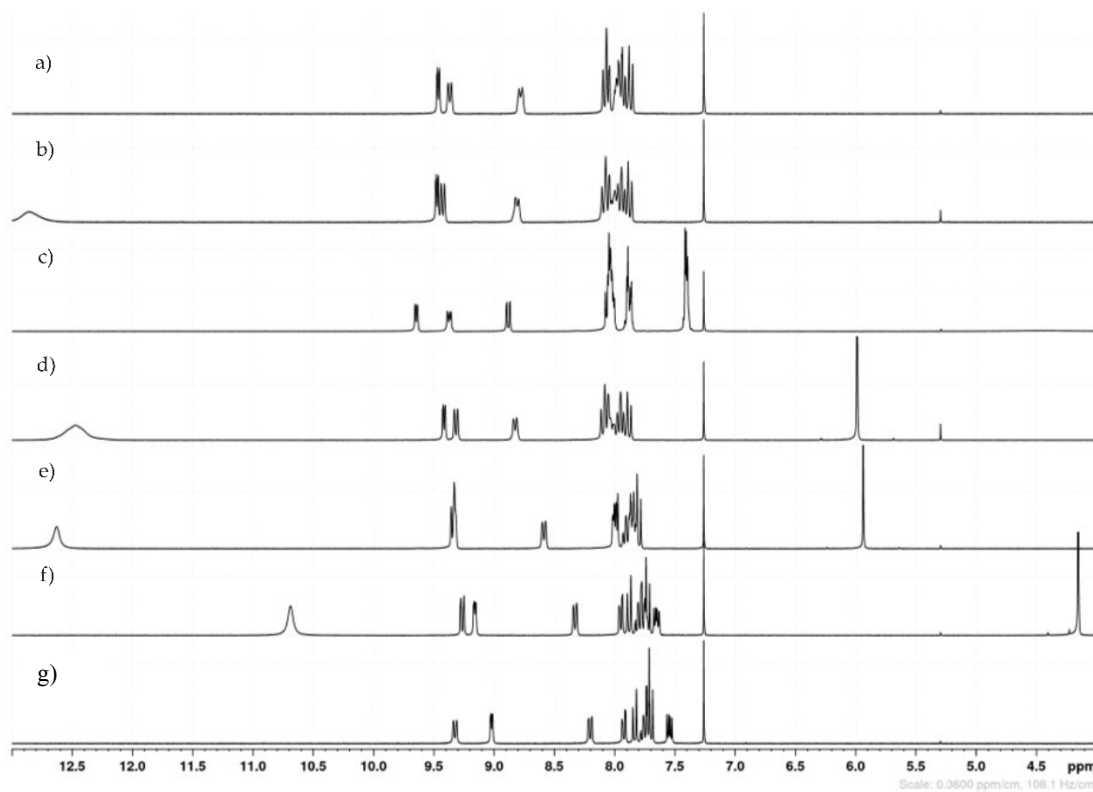


**Figure S13.**  $^1\text{H}$  NMR spectra of benzo[*h*]quinoline with 1:1 ratio of a) TFA b) TCA c) BSA d) DCA e) DBA f) CA and g) on its own ( $\text{CDCl}_3$ , 303 K, 300 MHz, 30 mM).

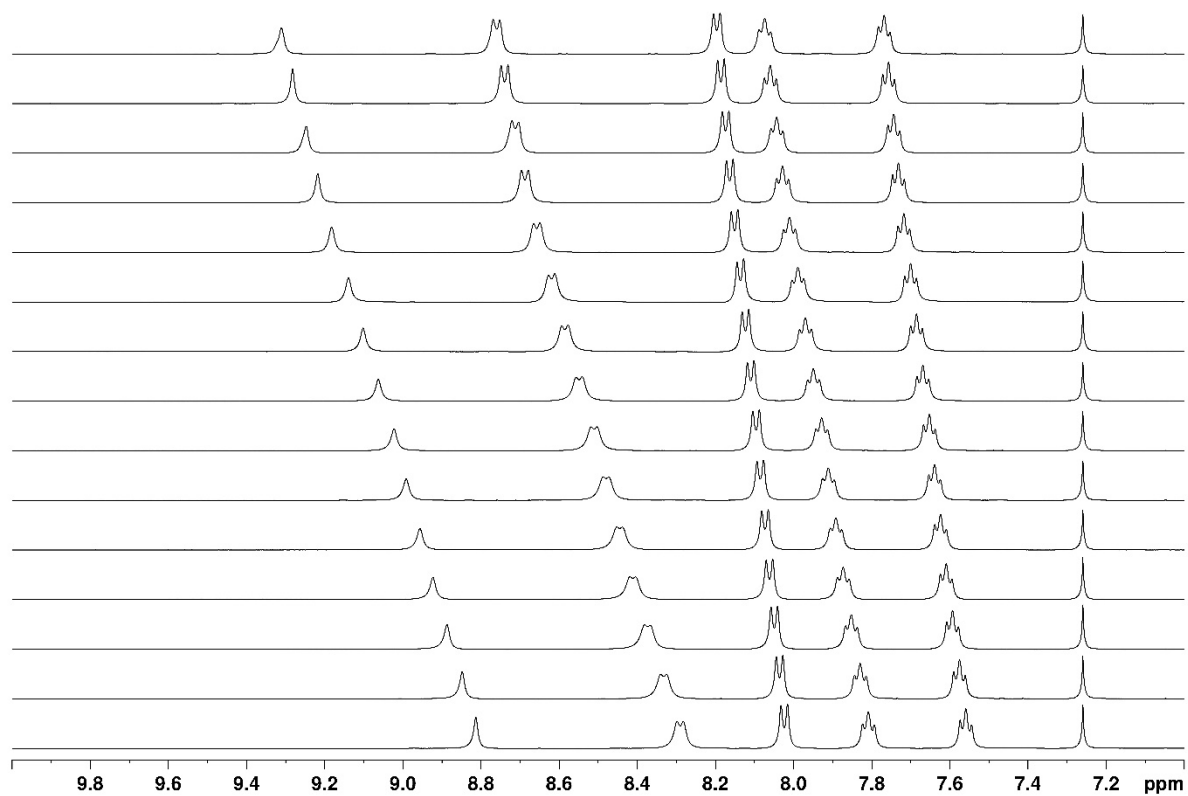


**Figure S14.** <sup>1</sup>H NMR spectra of acridine while titrating with TFA from 0.0 (bottom) to 1.4 (top spectrum) equivalence of the acid (CDCl<sub>3</sub>, 303 K, 500 MHz, 30 mM).

## 4. X-Ray Crystallography

The experimental and refinement details for complexes **1-14** are given below. All structures were measured using a Bruker-Nonius KappaCCD diffractometer with an APEX-II detector with graphite-monochromatized Mo- $K_{\alpha}$  ( $\lambda = 0.71073$  Å) radiation. Data collection and reduction were performed using the program *COLLECT*<sup>3</sup> and *HKL DENZO AND SCALEPACK*,<sup>4</sup> respectively, and the intensities were corrected for absorption using *SADABS*.<sup>5</sup> The structures were solved with intrinsic phasing (*SHELXT*)<sup>6</sup> and refined by full-matrix least squares on  $F^2$  using the *OLEX2* software,<sup>7</sup> which utilizes the *SHELXL-2015* module.<sup>8</sup> Non-hydrogen atoms were assigned anisotropic displacement parameters unless stated otherwise. Hydrogen atoms bonded to oxygen were located from Fourier difference maps and refined with an O–H distance restraint of approximately 0.84 Å. Other hydrogen atoms were placed in idealized positions and included as riding, with a value of 1.04 Å used for N–H bonds, which was based on an average of neutron diffraction values reported for this moiety with similarly hybridised neighbouring atoms.<sup>9</sup> Isotropic displacement parameters for all H atoms were constrained to multiples of the equivalent displacement parameters of their parent atoms with  $U_{\text{iso}}(\text{H}) = 1.2 U_{\text{eq}}(\text{parent atom})$ . The X-ray single crystal data and experimental details and CCDC numbers are given below.

### 4.1 X-Ray Experimental Details

Crystal data for **1** (obtained from vapour diffusion of dichloromethane and diisopropyl ether): CCDC-2000976,  $[\text{C}_9\text{H}_8\text{N}][\text{C}_2\text{F}_3\text{O}_2]$ ,  $M = 243.18 \text{ g mol}^{-1}$ , colourless plate,  $0.28 \times 0.14 \times 0.06 \text{ mm}^3$ , triclinic, space group  $P-1$ ,  $a = 4.7905(3) \text{ \AA}$ ,  $b = 10.1855(7) \text{ \AA}$ ,  $c = 11.2559(9) \text{ \AA}$ ,  $\alpha = 78.8360(10)^\circ$ ,  $\beta = 80.287(2)^\circ$ ,  $\gamma = 80.584(2)^\circ$ ,  $V = 526.21(6) \text{ \AA}^3$ ,  $Z = 2$ ,  $D_{\text{calc}} = 1.535 \text{ g cm}^{-3}$ ,  $F(000) = 248$ ,  $\mu = 0.14 \text{ mm}^{-1}$ ,  $T = 170(2) \text{ K}$ ,  $\theta_{\text{max}} = 26.2^\circ$ , 4832 total reflections, 1219 with  $I_o > 2\sigma(I_o)$ ,  $R_{\text{int}} = 0.049$ , 2095 data, 154 parameters, no restraints,  $\text{Goof} = 1.02$ ,  $R = 0.072$  and  $wR = 0.143 [I_o > 2\sigma(I_o)]$ ,  $R = 0.133$  and  $wR = 0.169$  (all reflections),  $0.40 < d\Delta\rho < -0.26 \text{ e\AA}^{-3}$ .

Crystal data for **2** (obtained from vapour diffusion of dichloromethane and diisopropyl ether): CCDC-2000977,  $[\text{C}_9\text{H}_8\text{N}][\text{C}_2\text{Cl}_3\text{O}_2]$ ,  $M = 292.53 \text{ g mol}^{-1}$ , colourless plate,  $0.50 \times 0.14 \times 0.08 \text{ mm}^3$ , monoclinic, space group  $P2_1/c$ ,  $a = 10.1155(6) \text{ \AA}$ ,  $b = 11.3509(4) \text{ \AA}$ ,  $c = 11.1128(5) \text{ \AA}$ ,  $\beta = 111.011(2)^\circ$ ,  $V = 1191.13(10) \text{ \AA}^3$ ,  $Z = 4$ ,  $D_{\text{calc}} = 1.631 \text{ g cm}^{-3}$ ,  $F(000) = 592$ ,  $\mu = 0.76 \text{ mm}^{-1}$ ,  $T = 170(2) \text{ K}$ ,  $\theta_{\text{max}} = 31.4^\circ$ , 13225 total reflections, 2587 with  $I_o > 2\sigma(I_o)$ ,  $R_{\text{int}} = 0.056$ , 3863 data, 154 parameters, no restraints,  $\text{Goof} = 1.05$ ,  $R = 0.055$  and  $wR = 0.107 [I_o > 2\sigma(I_o)]$ ,  $R = 0.095$  and  $wR = 0.121$  (all reflections),  $0.37 < d\Delta\rho < -0.35 \text{ e\AA}^{-3}$ .

Crystal data for **3** (obtained from slow evaporation of chloroform): CCDC-2000978,  $[\text{C}_9\text{H}_8\text{N}][\text{C}_6\text{H}_5\text{O}_3\text{S}]$ ,  $M = 287.32 \text{ g mol}^{-1}$ , colourless needle,  $0.41 \times 0.22 \times 0.21 \text{ mm}^3$ , monoclinic, space group  $P2_1/c$ ,  $a = 7.8573(9) \text{ \AA}$ ,  $b = 11.8280(15) \text{ \AA}$ ,  $c = 16.5782(19) \text{ \AA}$ ,  $\beta = 96.242(3)^\circ$ ,  $V = 1531.6(3) \text{ \AA}^3$ ,  $Z = 4$ ,  $D_{\text{calc}} = 1.246 \text{ g cm}^{-3}$ ,  $F(000) = 600$ ,  $\mu = 0.22 \text{ mm}^{-1}$ ,  $T = 170(2) \text{ K}$ ,  $\theta_{\text{max}} = 25.2^\circ$ , 8792 total reflections, 2127 with  $I_o > 2\sigma(I_o)$ ,  $R_{\text{int}} = 0.056$ , 2720 data, 181 parameters, no restraints,  $\text{Goof} = 1.07$ ,  $R = 0.082$  and  $wR = 0.198 [I_o > 2\sigma(I_o)]$ ,  $R = 0.103$  and  $wR = 0.210$  (all reflections),  $0.40 < d\Delta\rho < -0.56 \text{ e\AA}^{-3}$ .

Crystal data for **4** (obtained from vapour diffusion of dichloromethane and diisopropyl ether): CCDC-2000979,  $[\text{C}_{13}\text{H}_{10}\text{N}][\text{C}_2\text{F}_3\text{O}_2]$ ,  $M = 293.24 \text{ g mol}^{-1}$ , yellow block,  $0.43 \times 0.30 \times 0.26 \text{ mm}^3$ , monoclinic, space group  $P2_1/c$ ,  $a = 9.5335(3) \text{ \AA}$ ,  $b = 18.6879(5) \text{ \AA}$ ,  $c = 7.1523(2) \text{ \AA}$ ,  $\beta = 96.999(2)^\circ$ ,  $V = 1264.77(6) \text{ \AA}^3$ ,  $Z = 4$ ,  $D_{\text{calc}} = 1.540 \text{ g cm}^{-3}$ ,  $F(000) = 600$ ,  $\mu = 0.13 \text{ mm}^{-1}$ ,  $T = 170(2) \text{ K}$ ,  $\theta_{\text{max}} = 26.3^\circ$ , 8996 total reflections, 2064 with  $I_o > 2\sigma(I_o)$ ,  $R_{\text{int}} = 0.030$ , 2545 data, 190 parameters, no restraints,  $\text{Goof} = 1.04$ ,  $R = 0.049$  and  $wR = 0.118 [I_o > 2\sigma(I_o)]$ ,  $R = 0.061$  and  $wR = 0.126$  (all reflections),  $0.39 < d\Delta\rho < -0.28 \text{ e\AA}^{-3}$ .

Crystal data for **5** (obtained from vapour diffusion of dichloromethane and diisopropyl ether): CCDC-2000980,  $[\text{C}_{13}\text{H}_{10}\text{N}][\text{C}_2\text{Cl}_3\text{O}_2]$ ,  $M = 342.59 \text{ g mol}^{-1}$ , yellow plate,  $0.14 \times 0.13 \times 0.06 \text{ mm}^3$ , triclinic, space group  $P-1$ ,  $a = 6.8497(4) \text{ \AA}$ ,  $b = 9.3744(8) \text{ \AA}$ ,  $c = 12.0307(10) \text{ \AA}$ ,  $\alpha = 76.517(3)^\circ$ ,  $\beta = 74.637(5)^\circ$ ,  $\gamma = 79.462(5)^\circ$ ,  $V = 718.31(10) \text{ \AA}^3$ ,  $Z = 2$ ,  $D_{\text{calc}} = 1.584 \text{ g cm}^{-3}$ ,  $F(000) = 348$ ,  $\mu = 0.64 \text{ mm}^{-1}$ ,  $T = 170(2) \text{ K}$ ,  $\theta_{\text{max}} = 26.3^\circ$ , 6478 total reflections, 2068 with  $I_o > 2\sigma(I_o)$ ,  $R_{\text{int}} = 0.035$ , 2875 data, 190 parameters, no restraints,  $\text{Goof} = 1.04$ ,  $R = 0.048$  and  $wR = 0.098 [I_o > 2\sigma(I_o)]$ ,  $R = 0.075$  and  $wR = 0.107$  (all reflections),  $0.24 < d\Delta\rho < -0.30 \text{ e\AA}^{-3}$ .

Crystal data for **6** (obtained from vapour diffusion of dichloromethane and diisopropyl ether): CCDC-2000981,  $[\text{C}_{13}\text{H}_{10}\text{N}][\text{C}_6\text{H}_5\text{O}_3\text{S}]$ ,  $M = 337.38 \text{ g mol}^{-1}$ , yellow block,  $0.35 \times 0.32 \times 0.32 \text{ mm}^3$ , monoclinic, space group  $P2_1/c$ ,  $a = 7.1261(2) \text{ \AA}$ ,  $b = 9.7581(4) \text{ \AA}$ ,  $c = 22.8711(8) \text{ \AA}$ ,  $\beta = 90.978(2)^\circ$ ,  $V = 1590.16(10) \text{ \AA}^3$ ,  $Z = 4$ ,  $D_{\text{calc}} = 1.409 \text{ g cm}^{-3}$ ,  $F(000) = 704$ ,  $\mu = 0.22 \text{ mm}^{-1}$ ,  $T = 170(2) \text{ K}$ ,  $\theta_{\text{max}} = 26.3^\circ$ , 10920 total reflections, 2497 with  $I_o > 2\sigma(I_o)$ ,  $R_{\text{int}} = 0.042$ , 3197 data, 217 parameters, no restraints,  $\text{Goof} = 1.04$ ,  $R = 0.048$  and  $wR = 0.112 [I_o > 2\sigma(I_o)]$ ,  $R = 0.065$  and  $wR = 0.121$  (all reflections),  $0.47 < d\Delta\rho < -0.33 \text{ e\AA}^{-3}$ .

Crystal data for **7** (obtained from vapour diffusion of chloroform and hexane): CCDC-2000982,  $[\text{C}_{13}\text{H}_{10}\text{N}][\text{C}_2\text{HCl}_2\text{O}_2] \cdot \text{C}_2\text{H}_2\text{Cl}_2\text{O}_2$ ,  $M = 437.08 \text{ g mol}^{-1}$ , yellow plate,  $0.26 \times 0.23 \times 0.12 \text{ mm}^3$ , triclinic, space group  $P-1$ ,  $a =$

6.0822(3) Å,  $b = 7.8975(4)$  Å,  $c = 9.9912(19)$  Å,  $\alpha = 104.058(3)^\circ$ ,  $\beta = 96.799(2)^\circ$ ,  $\gamma = 95.159(3)^\circ$ ,  $V = 458.75(9)$  Å<sup>3</sup>,  $Z = 1$ ,  $D_{\text{calc}} = 1.582$  gcm<sup>-3</sup>,  $F(000) = 222$ ,  $\mu = 0.67$  mm<sup>-1</sup>,  $T = 170(2)$  K,  $\theta_{\text{max}} = 25.1^\circ$ , 3384 total reflections, 1433 with  $I_o > 2\sigma(I_o)$ ,  $R_{\text{int}} = 0.023$ , 1624 data, 118 parameters, no restraints,  $\text{Goof} = 1.01$ ,  $R = 0.046$  and  $wR = 0.119$  [ $I_o > 2\sigma(I_o)$ ],  $R = 0.052$  and  $wR = 0.121$  (all reflections),  $0.28 < d\Delta\rho < -0.41$  eÅ<sup>-3</sup>.

Crystal data for **8** (obtained from vapour diffusion of chloroform and hexane): CCDC-2000983, [C<sub>13</sub>H<sub>10</sub>N][C<sub>2</sub>HBr<sub>2</sub>O<sub>2</sub>] $\cdot$ C<sub>2</sub>H<sub>2</sub>Br<sub>2</sub>O<sub>2</sub>,  $M = 614.92$  gmol<sup>-1</sup>, yellow plate,  $0.23 \times 0.21 \times 0.10$  mm<sup>3</sup>, triclinic, space group  $P-1$ ,  $a = 6.3247(2)$  Å,  $b = 7.9047(4)$  Å,  $c = 10.1134(5)$  Å,  $\alpha = 103.479(2)^\circ$ ,  $\beta = 96.829(3)^\circ$ ,  $\gamma = 95.388(3)^\circ$ ,  $V = 484.31(4)$  Å<sup>3</sup>,  $Z = 1$ ,  $D_{\text{calc}} = 2.108$  gcm<sup>-3</sup>,  $F(000) = 294$ ,  $\mu = 8.33$  mm<sup>-1</sup>,  $T = 170(2)$  K,  $\theta_{\text{max}} = 26.3^\circ$ , 4378 total reflections, 1622 with  $I_o > 2\sigma(I_o)$ ,  $R_{\text{int}} = 0.036$ , 1936 data, 118 parameters, no restraints,  $\text{Goof} = 1.03$ ,  $R = 0.041$  and  $wR = 0.090$  [ $I_o > 2\sigma(I_o)$ ],  $R = 0.052$  and  $wR = 0.096$  (all reflections),  $0.46 < d\Delta\rho < -0.90$  eÅ<sup>-3</sup>.

Crystal data for **9** (obtained from vapour diffusion of chloroform and hexane): CCDC-2000984, [C<sub>13</sub>H<sub>10</sub>N][C<sub>2</sub>H<sub>2</sub>ClO<sub>2</sub>],  $M = 273.71$  gmol<sup>-1</sup>, yellow needle,  $0.22 \times 0.17 \times 0.14$  mm<sup>3</sup>, triclinic, space group  $P-1$ ,  $a = 7.2478(4)$  Å,  $b = 8.8083(3)$  Å,  $c = 11.5321(6)$  Å,  $\alpha = 69.550(1)^\circ$ ,  $\beta = 73.313(2)^\circ$ ,  $\gamma = 67.418(1)^\circ$ ,  $V = 626.90(5)$  Å<sup>3</sup>,  $Z = 2$ ,  $D_{\text{calc}} = 1.450$  gcm<sup>-3</sup>,  $F(000) = 284$ ,  $\mu = 0.30$  mm<sup>-1</sup>,  $T = 170(2)$  K,  $\theta_{\text{max}} = 26.3^\circ$ , 5222 total reflections, 1953 with  $I_o > 2\sigma(I_o)$ ,  $R_{\text{int}} = 0.036$ , 2513 data, 172 parameters, no restraints,  $\text{Goof} = 1.02$ ,  $R = 0.050$  and  $wR = 0.116$  [ $I_o > 2\sigma(I_o)$ ],  $R = 0.070$  and  $wR = 0.127$  (all reflections),  $0.28 < d\Delta\rho < -0.34$  eÅ<sup>-3</sup>.

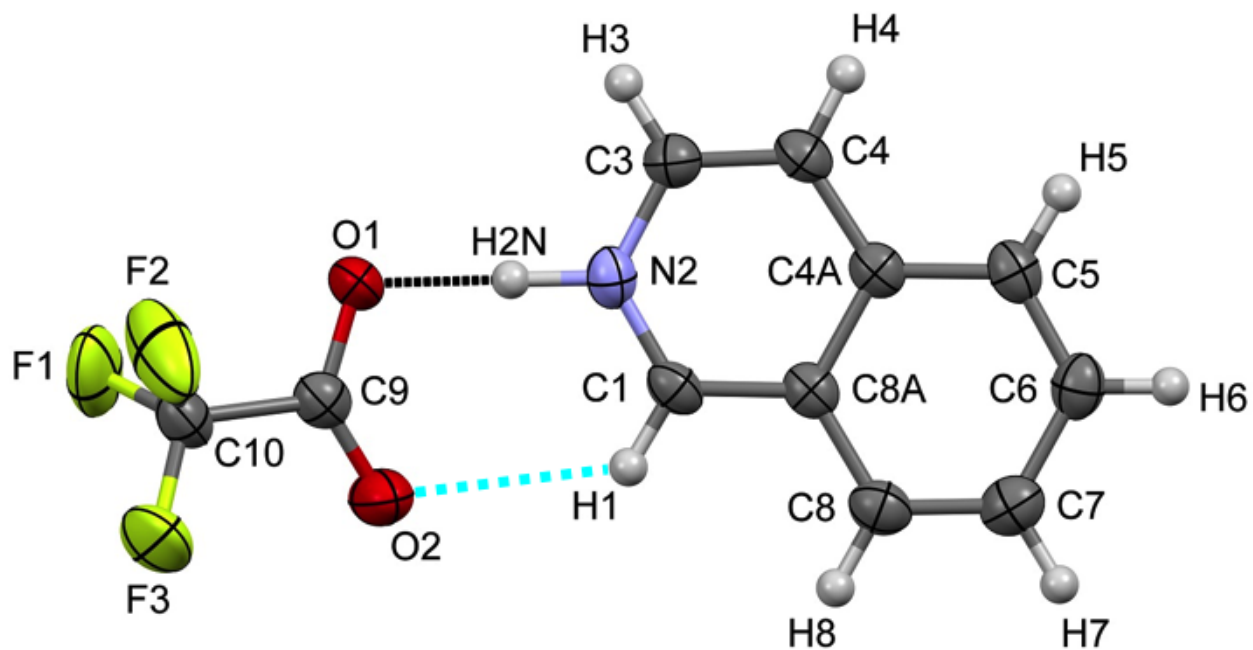
Crystal data for **10** (obtained from vapour diffusion of dichloromethane and diisopropyl ether): CCDC-2000985, [C<sub>13</sub>H<sub>10</sub>N][C<sub>2</sub>F<sub>3</sub>O<sub>2</sub>],  $M = 293.24$  gmol<sup>-1</sup>, colourless plate,  $0.31 \times 0.21 \times 0.05$  mm<sup>3</sup>, monoclinic, space group  $P2_1/n$ ,  $a = 10.0948(10)$  Å,  $b = 5.0687(3)$  Å,  $c = 24.9448(19)$  Å,  $\beta = 90.411(3)^\circ$ ,  $V = 1276.33(18)$  Å<sup>3</sup>,  $Z = 4$ ,  $D_{\text{calc}} = 1.526$  gcm<sup>-3</sup>,  $F(000) = 600$ ,  $\mu = 0.13$  mm<sup>-1</sup>,  $T = 170(2)$  K,  $\theta_{\text{max}} = 25.2^\circ$ , 4994 total reflections, 1351 with  $I_o > 2\sigma(I_o)$ ,  $R_{\text{int}} = 0.055$ , 2203 data, 190 parameters, no restraints,  $\text{Goof} = 1.02$ ,  $R = 0.058$  and  $wR = 0.136$  [ $I_o > 2\sigma(I_o)$ ],  $R = 0.110$  and  $wR = 0.163$  (all reflections),  $0.41 < d\Delta\rho < -0.33$  eÅ<sup>-3</sup>.

Crystal data for **11** (obtained from vapour diffusion of dichloromethane and diisopropyl ether): CCDC-2000986, [C<sub>13</sub>H<sub>10</sub>N][C<sub>2</sub>Cl<sub>3</sub>O<sub>2</sub>],  $M = 342.59$  gmol<sup>-1</sup>, colourless block,  $0.26 \times 0.23 \times 0.22$  mm<sup>3</sup>, monoclinic, space group  $P2_1/n$ ,  $a = 6.6910(2)$  Å,  $b = 24.1354(7)$  Å,  $c = 18.5026(5)$  Å,  $\beta = 92.611(2)^\circ$ ,  $V = 2984.88(15)$  Å<sup>3</sup>,  $Z = 8$ ,  $D_{\text{calc}} = 1.525$  gcm<sup>-3</sup>,  $F(000) = 1392$ ,  $\mu = 0.62$  mm<sup>-1</sup>,  $T = 170(2)$  K,  $\theta_{\text{max}} = 25.3^\circ$ , 13612 total reflections, 4025 with  $I_o > 2\sigma(I_o)$ ,  $R_{\text{int}} = 0.029$ , 5345 data, 379 parameters, no restraints,  $\text{Goof} = 1.08$ ,  $R = 0.062$  and  $wR = 0.161$  [ $I_o > 2\sigma(I_o)$ ],  $R = 0.082$  and  $wR = 0.173$  (all reflections),  $1.41 < d\Delta\rho < -0.97$  eÅ<sup>-3</sup>.

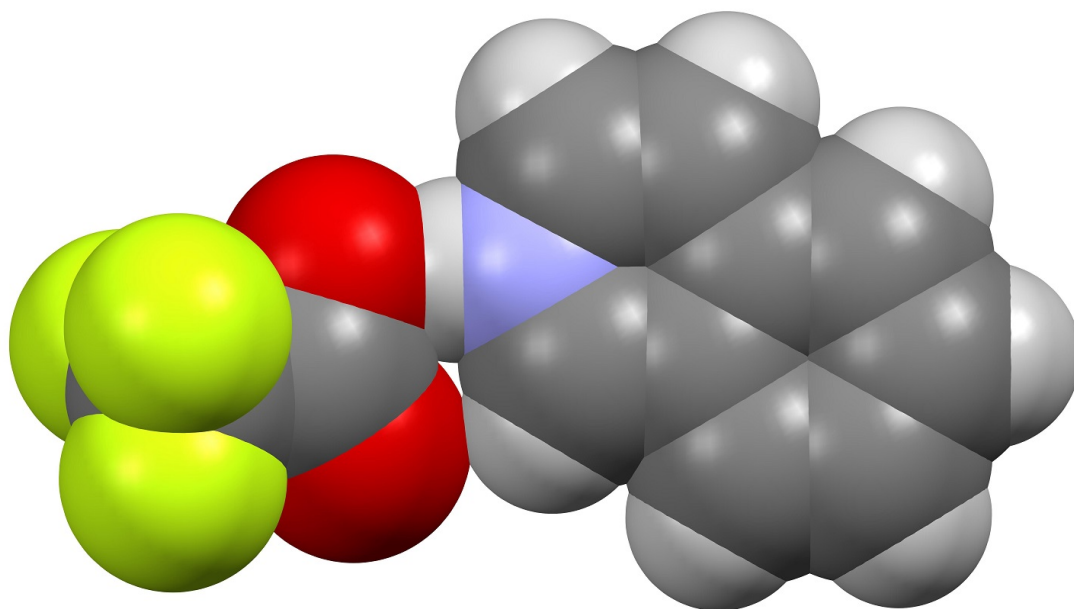
Crystal data for **12** (obtained from slow evaporation of chloroform): CCDC-2000987, [C<sub>13</sub>H<sub>10</sub>N][C<sub>6</sub>H<sub>5</sub>O<sub>3</sub>S],  $M = 337.38$  gmol<sup>-1</sup>, colourless plate,  $0.25 \times 0.23 \times 0.12$  mm<sup>3</sup>, monoclinic, space group  $P2_1/c$ ,  $a = 7.4888(2)$  Å,  $b = 12.3779(4)$  Å,  $c = 19.0995(7)$  Å,  $\beta = 97.448(2)^\circ$ ,  $V = 1755.50(10)$  Å<sup>3</sup>,  $Z = 4$ ,  $D_{\text{calc}} = 1.277$  gcm<sup>-3</sup>,  $F(000) = 704$ ,  $\mu = 0.20$  mm<sup>-1</sup>,  $T = 170(2)$  K,  $\theta_{\text{max}} = 25.3^\circ$ , 13309 total reflections, 2278 with  $I_o > 2\sigma(I_o)$ ,  $R_{\text{int}} = 0.050$ , 3168 data, 217 parameters, no restraints,  $\text{Goof} = 1.02$ ,  $R = 0.058$  and  $wR = 0.142$  [ $I_o > 2\sigma(I_o)$ ],  $R = 0.087$  and  $wR = 0.159$  (all reflections),  $0.37 < d\Delta\rho < -0.69$  eÅ<sup>-3</sup>.

Crystal data for **13** (obtained from vapour diffusion of chloroform and hexane): CCDC-2000988, [C<sub>13</sub>H<sub>10</sub>N][C<sub>2</sub>HCl<sub>2</sub>O<sub>2</sub>] $\cdot$ C<sub>2</sub>H<sub>2</sub>Cl<sub>2</sub>O<sub>2</sub>,  $M = 437.08$  gmol<sup>-1</sup>, colourless block,  $0.26 \times 0.22 \times 0.22$  mm<sup>3</sup>, monoclinic, space group  $P2_1/c$ ,  $a = 8.4155(3)$  Å,  $b = 11.3195(5)$  Å,  $c = 19.7432(8)$  Å,  $\beta = 92.939(2)^\circ$ ,  $V = 1878.25(13)$  Å<sup>3</sup>,  $Z = 4$ ,  $D_{\text{calc}} = 1.546$  gcm<sup>-3</sup>,  $F(000) = 888$ ,  $\mu = 0.65$  mm<sup>-1</sup>,  $T = 170(2)$  K,  $\theta_{\text{max}} = 26.3^\circ$ , 10664 total reflections, 2567 with  $I_o > 2\sigma(I_o)$ ,  $R_{\text{int}} = 0.032$ , 3787 data, 239 parameters, no restraints,  $\text{Goof} = 1.01$ ,  $R = 0.050$  and  $wR = 0.109$  [ $I_o > 2\sigma(I_o)$ ],  $R = 0.082$  and  $wR = 0.124$  (all reflections),  $0.34 < d\Delta\rho < -0.38$  eÅ<sup>-3</sup>.

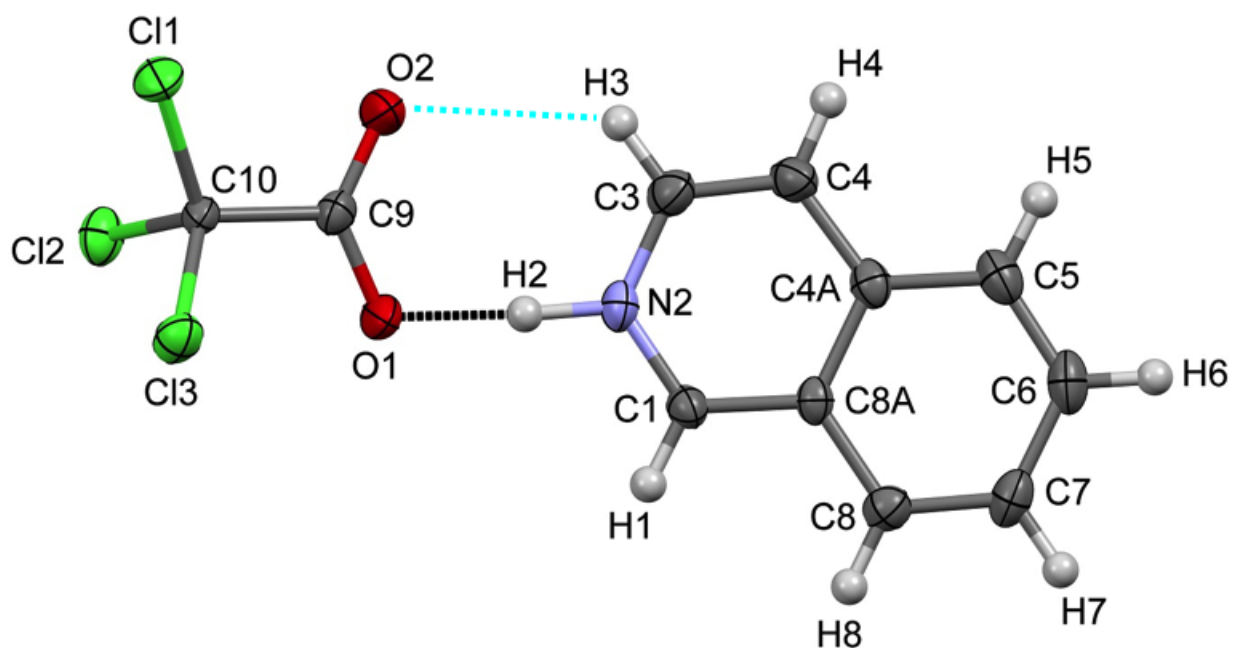
Crystal data for **14** (obtained from vapour diffusion of chloroform and hexane): CCDC-2000989, [C<sub>13</sub>H<sub>10</sub>N][C<sub>2</sub>HBr<sub>2</sub>O<sub>2</sub>] $\cdot$ C<sub>2</sub>H<sub>2</sub>Br<sub>2</sub>O<sub>2</sub>,  $M = 614.92$  gmol<sup>-1</sup>, colourless needle,  $0.40 \times 0.12 \times 0.08$  mm<sup>3</sup>, orthorhombic, space group  $P2_12_12_1$ ,  $a = 4.3451(2)$  Å,  $b = 19.0711(5)$  Å,  $c = 23.2876(6)$  Å,  $V = 1929.75(11)$  Å<sup>3</sup>,  $Z = 4$ ,  $D_{\text{calc}} = 2.117$  gcm<sup>-3</sup>,  $F(000) = 1176$ ,  $\mu = 8.36$  mm<sup>-1</sup>,  $T = 170(2)$  K,  $\theta_{\text{max}} = 26.3^\circ$ , 18405 total reflections, 3508 with  $I_o > 2\sigma(I_o)$ ,  $R_{\text{int}} = 0.044$ , 3887 data, 235 parameters, no restraints,  $\text{Goof} = 1.02$ ,  $R = 0.028$  and  $wR = 0.057$  [ $I_o > 2\sigma(I_o)$ ],  $R = 0.035$  and  $wR = 0.060$  (all reflections),  $0.75 < d\Delta\rho < -0.55$  eÅ<sup>-3</sup>.



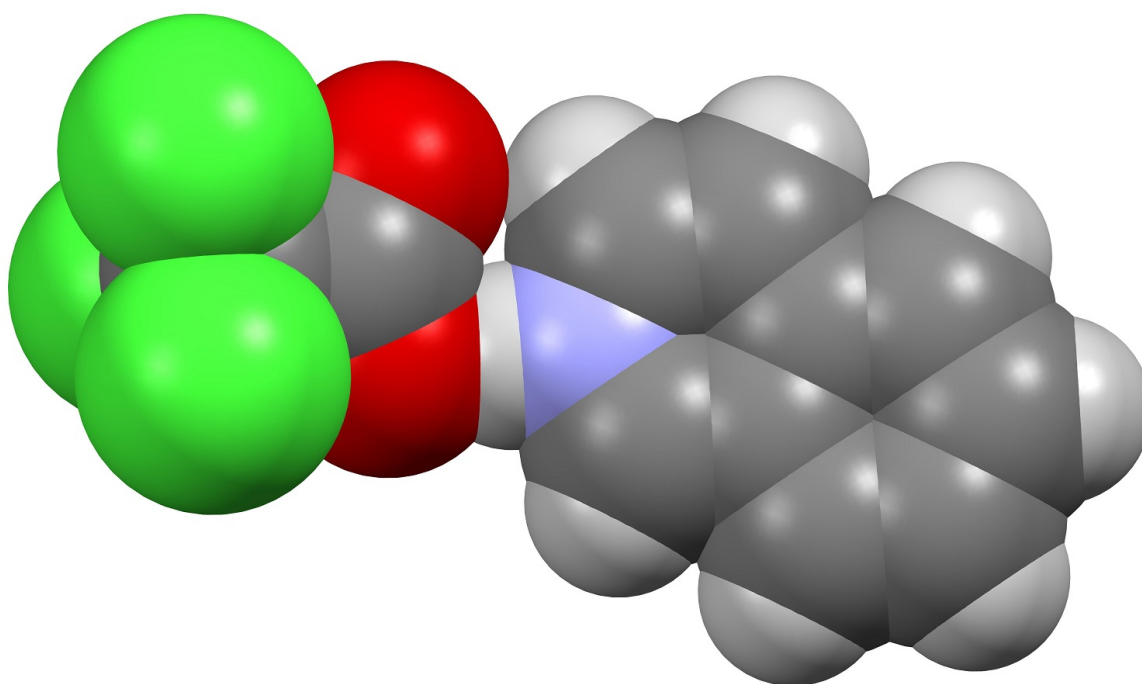
**Figure S15.** Displacement ellipsoid plot of **1**. Displacement ellipsoids are drawn at the 50% probability level. The black-dotted line is N–H···O hydrogen bond and light blue-dotted line represents weak intermolecular C–H···O interaction.



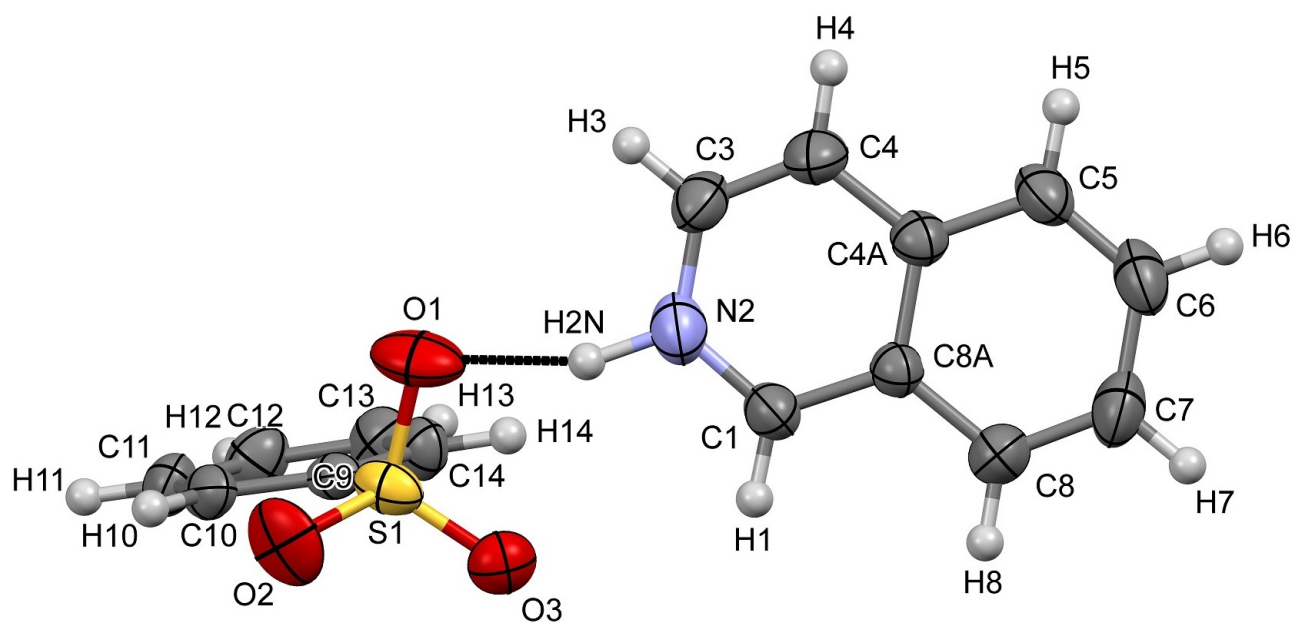
**Figure S16.** Space-filling model of **1**.



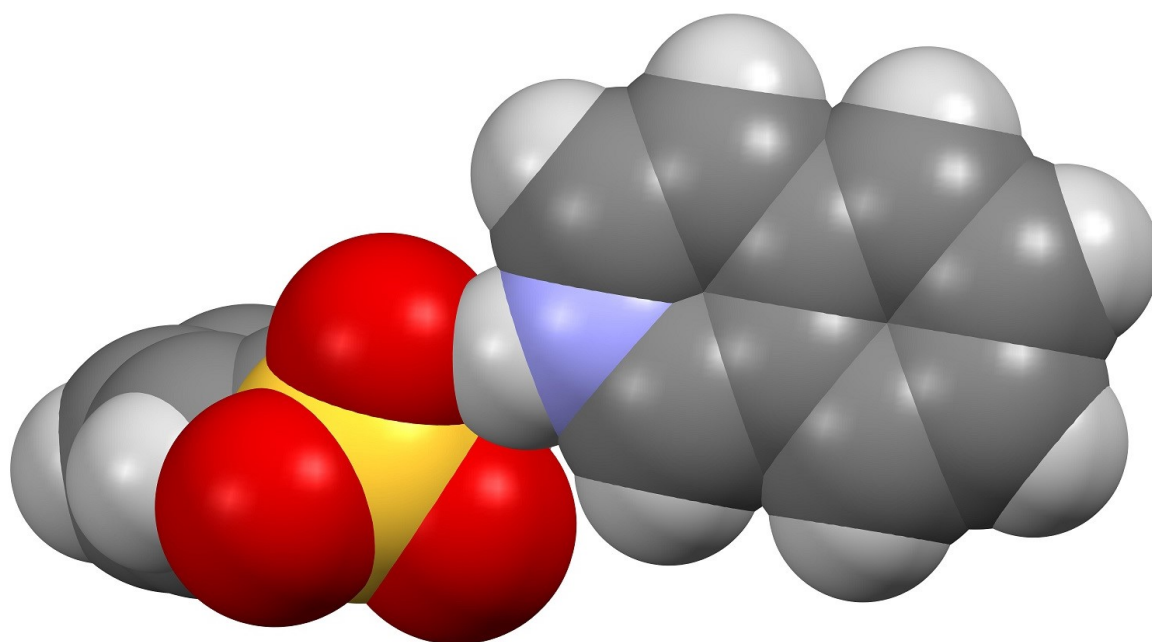
**Figure S17.** Displacement ellipsoid plot of **2**. Displacement ellipsoids are drawn at the 50% probability level. The black-dotted line is N–H...O hydrogen bond and light blue-dotted line represents weak intermolecular C–H...O interaction.



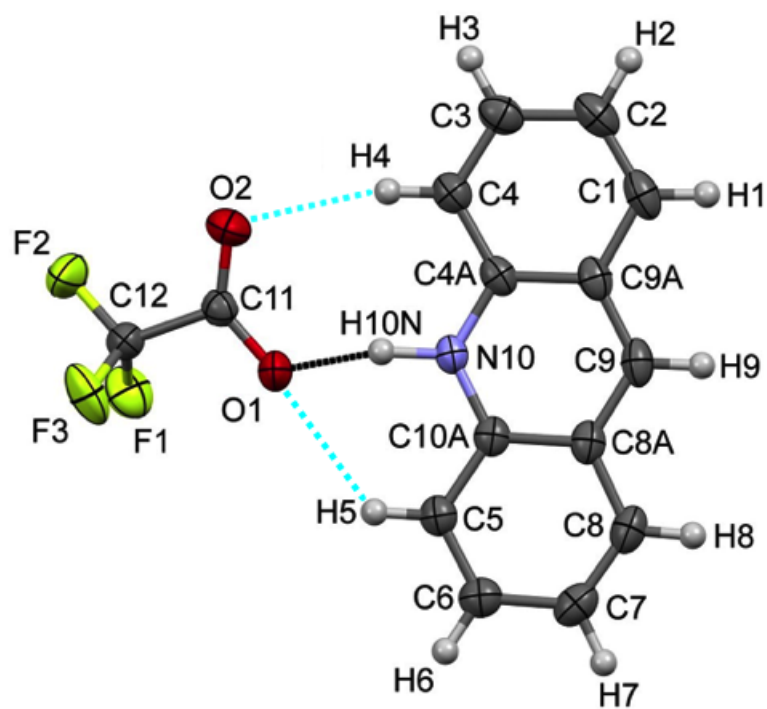
**Figure S18.** Space-filling model of **2**.



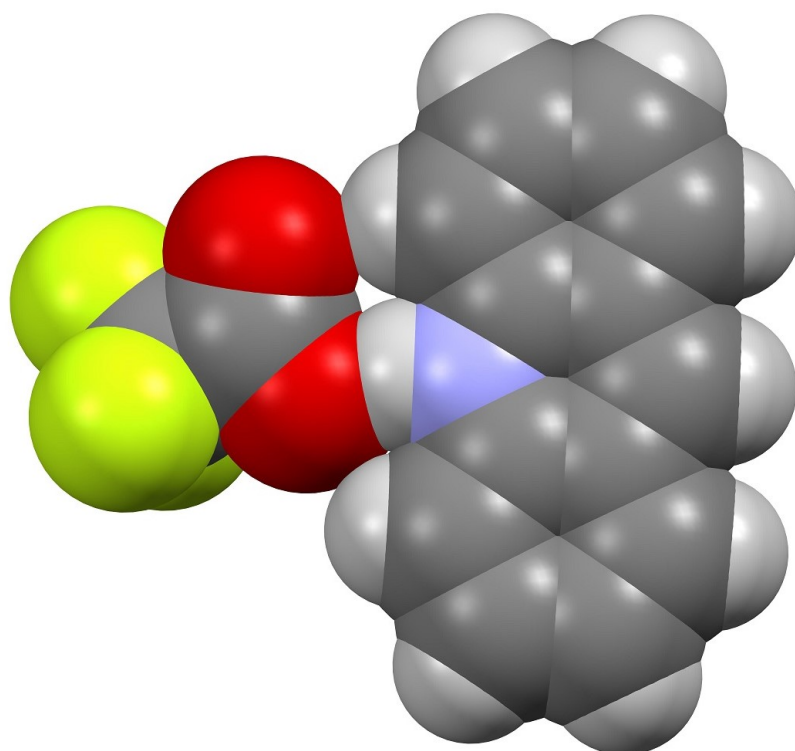
**Figure S19.** Displacement ellipsoid plot of **3**. Displacement ellipsoids are drawn at the 50% probability level. The black-dotted line represents N-H...O hydrogen bond.



**Figure S20.** Space-filling model of **3**.

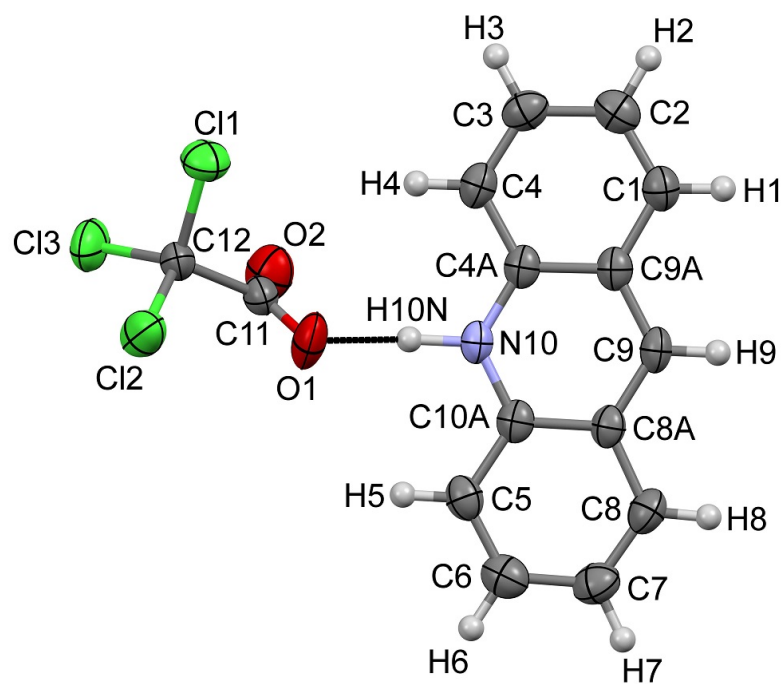


**Figure S21.** Displacement ellipsoid plot of **4**. Displacement ellipsoids are drawn at the 50% probability level. The black-dotted line is N–H $\cdots$ O hydrogen bond and light blue-dotted lines represent weak intermolecular C–H $\cdots$ O interactions.

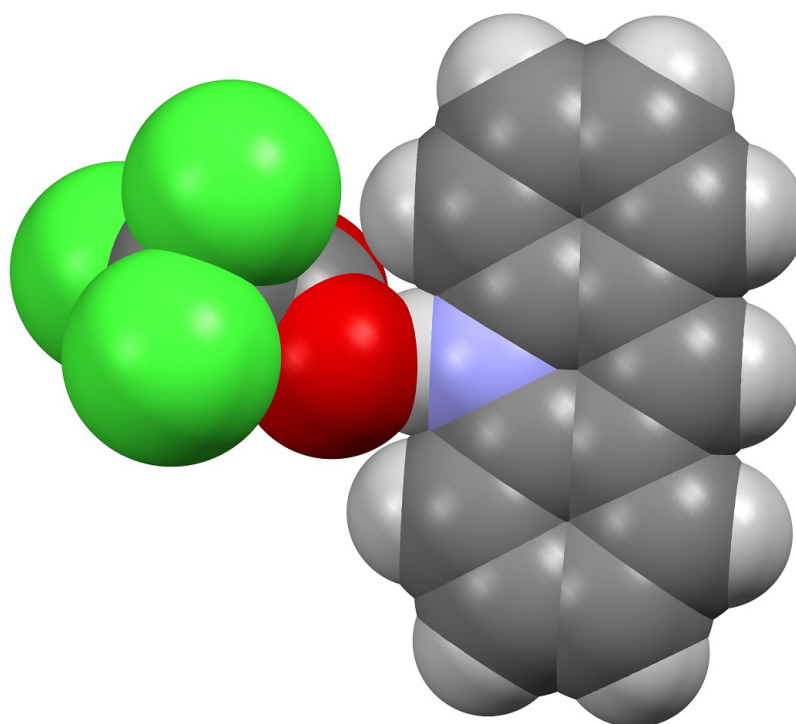


**Figure S22.** Space-filling model of **4**.

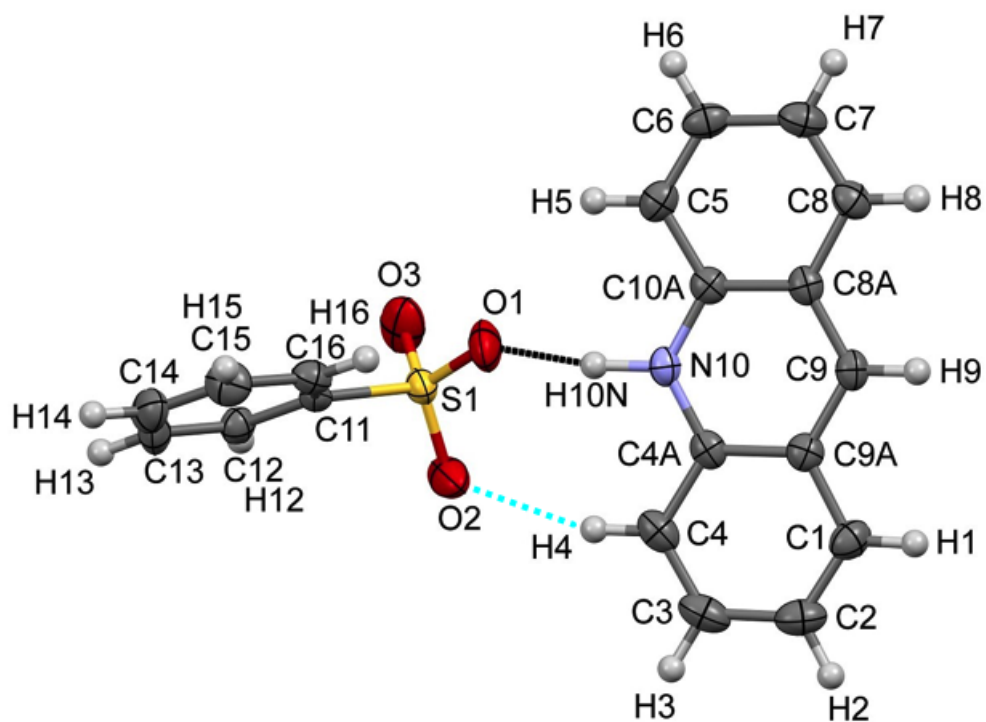




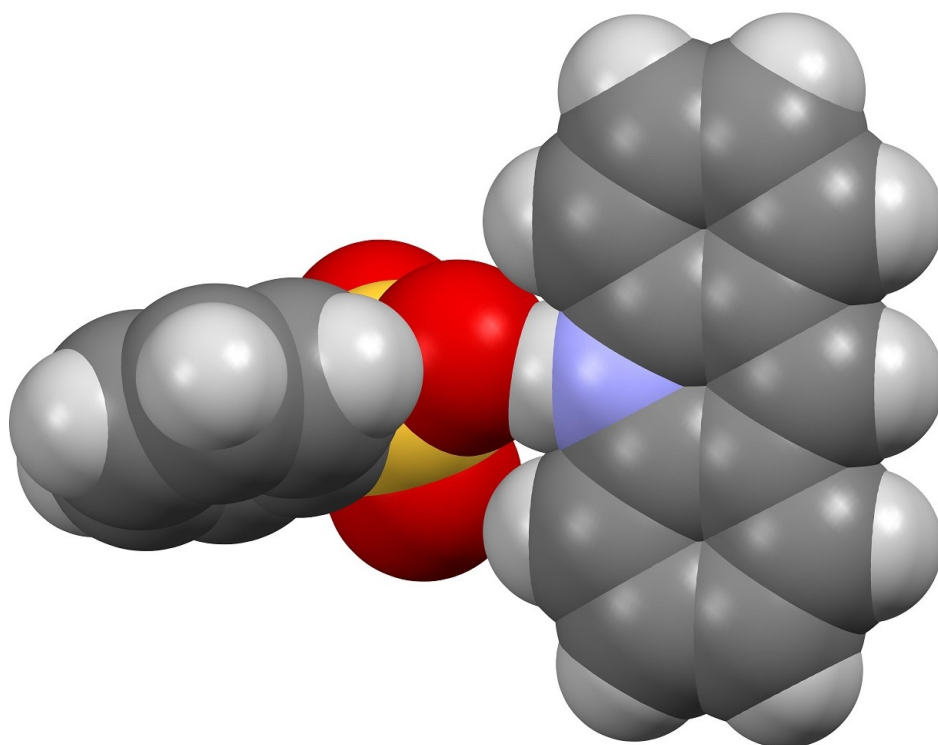
**Figure S23.** Displacement ellipsoid plot of **5**. Displacement ellipsoids are drawn at the 50% probability level. The black-dotted line represents N-H...O hydrogen bond.



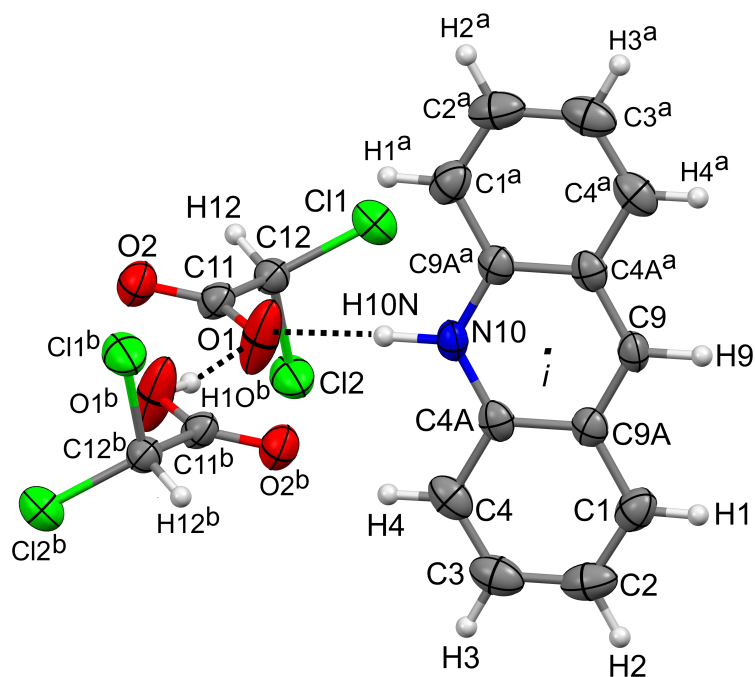
**Figure S24.** Space-filling model of **5**.



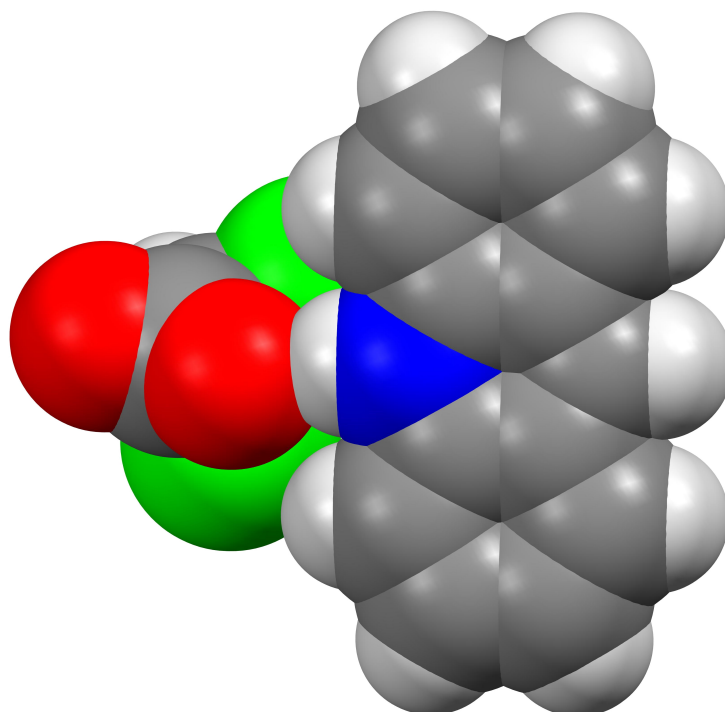
**Figure S25.** Displacement ellipsoid plot of **6**. Displacement ellipsoids are drawn at the 50% probability level. The black-dotted line represents N-H...O hydrogen bond and light blue-dotted line the weak intermolecular C-H...O interaction.



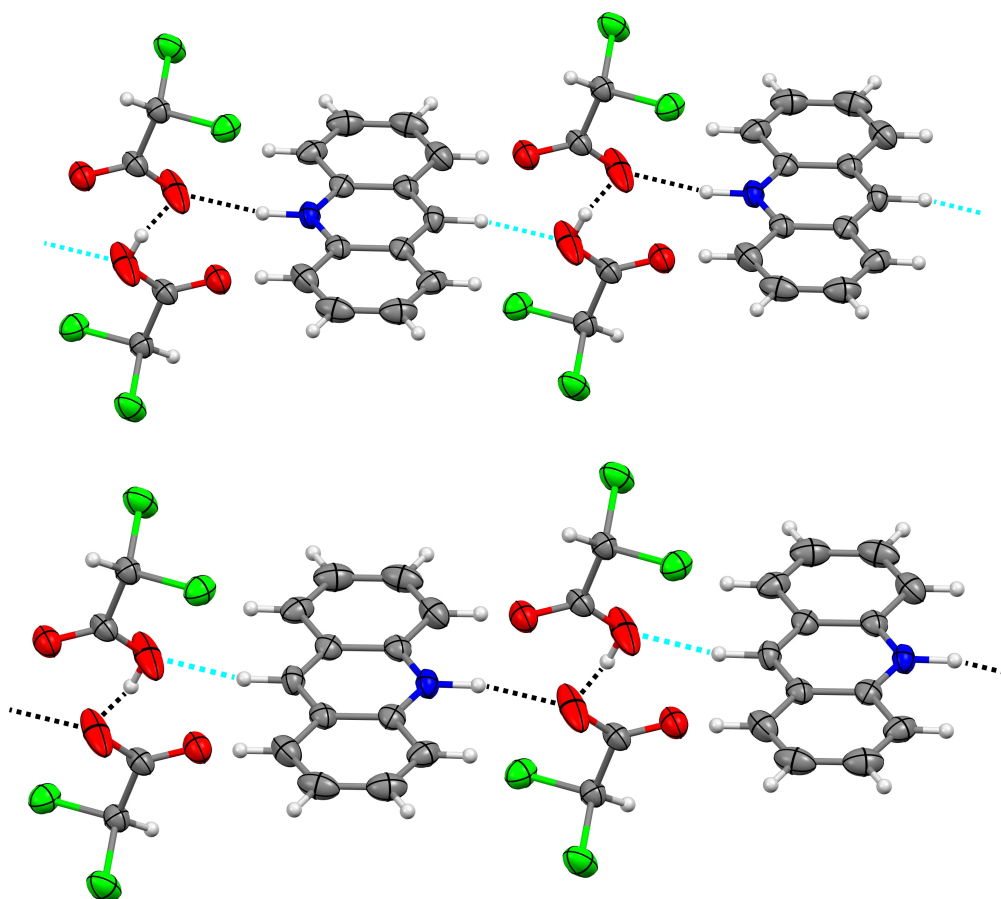
**Figure S26.** Space-filling model of **6**.



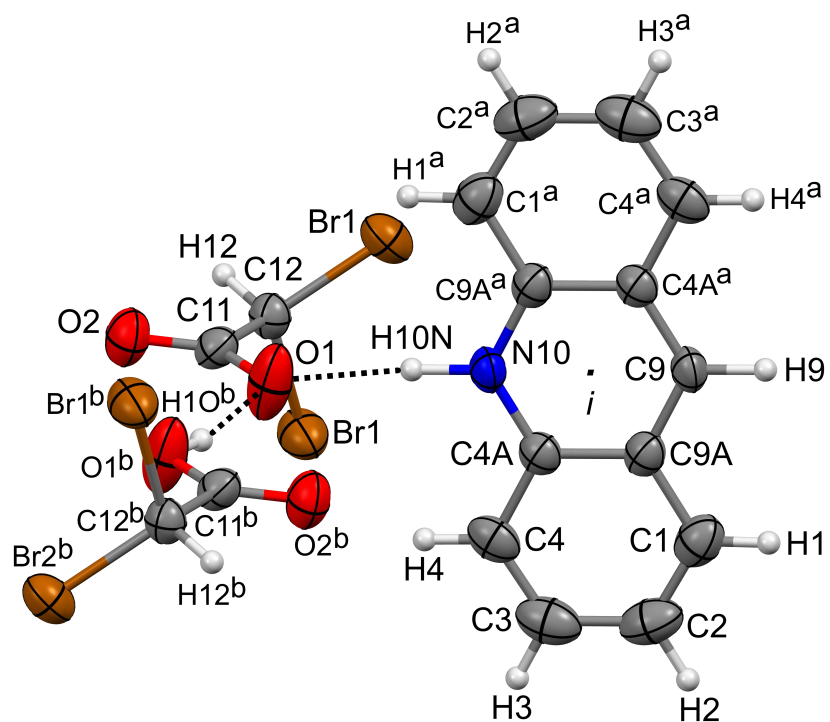
**Figure S27.** Displacement ellipsoid plot of **7**. Displacement ellipsoids are drawn at the 50% probability level. Only one disorder orientation is depicted for clarity. The black-dotted lines represent N-H...O and O-H...O hydrogen bonds, respectively (symmetry operator:  $a = -x, 1 - y, -z$ ;  $b = -x, 1 - y, 1 - z$ ).



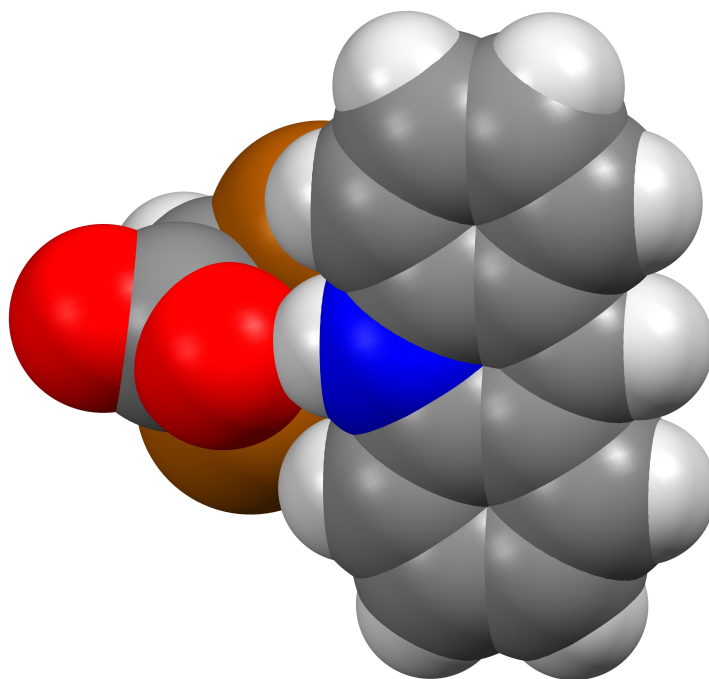
**Figure S28.** Space-filling model of **7** (one DCA molecule has been omitted for clarity).



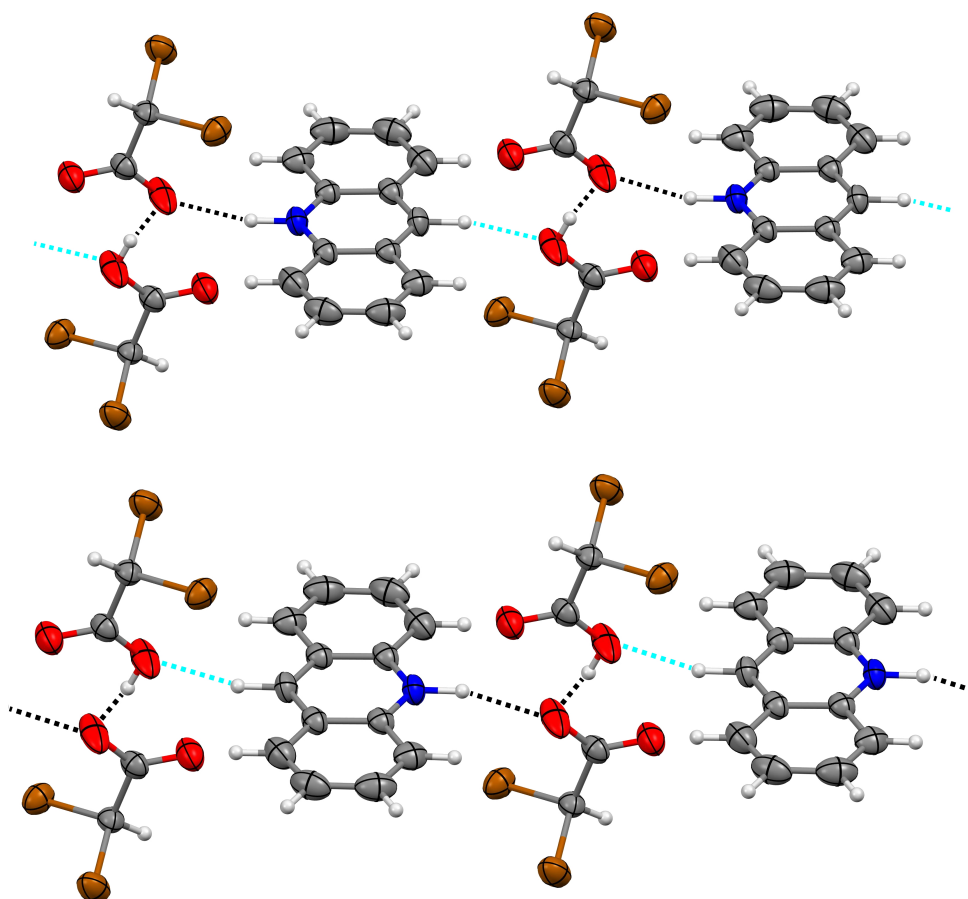
**Figure S29.** The individual disorder orientations in the X-ray structure of 7. Displacement ellipsoids are drawn at the 50% probability level. The black-dotted lines are N-H...O/O-H...O hydrogen bonds and light blue-dotted lines represent weak intermolecular C-H...O interactions.



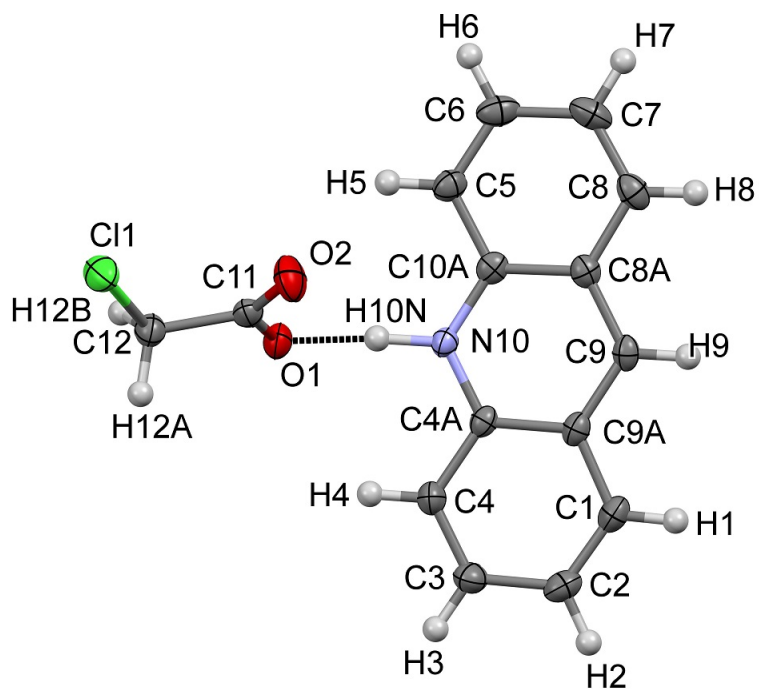
**Figure S30.** Displacement ellipsoid plot of **8**. Displacement ellipsoids are drawn at the 50% probability level. Only one disorder orientation is depicted for clarity. The black-dotted lines represent N–H···O and O–H···O hydrogen bonds, respectively (symmetry operator:  $a = -x, 1 - y, -z$ ;  $b = -x, 1 - y, 1 - z$ ).



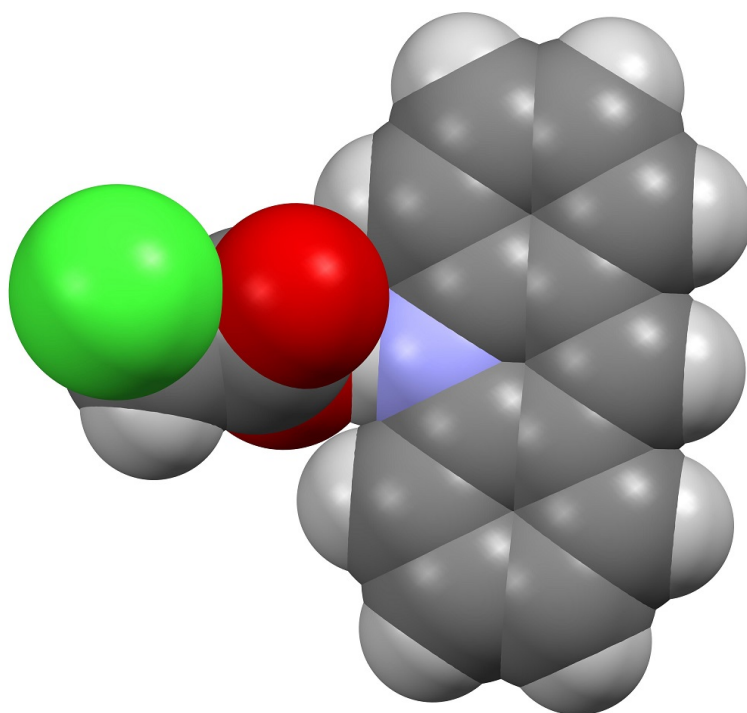
**Figure S31.** Space-filling model of **8** (one DBA molecule has been omitted for clarity).



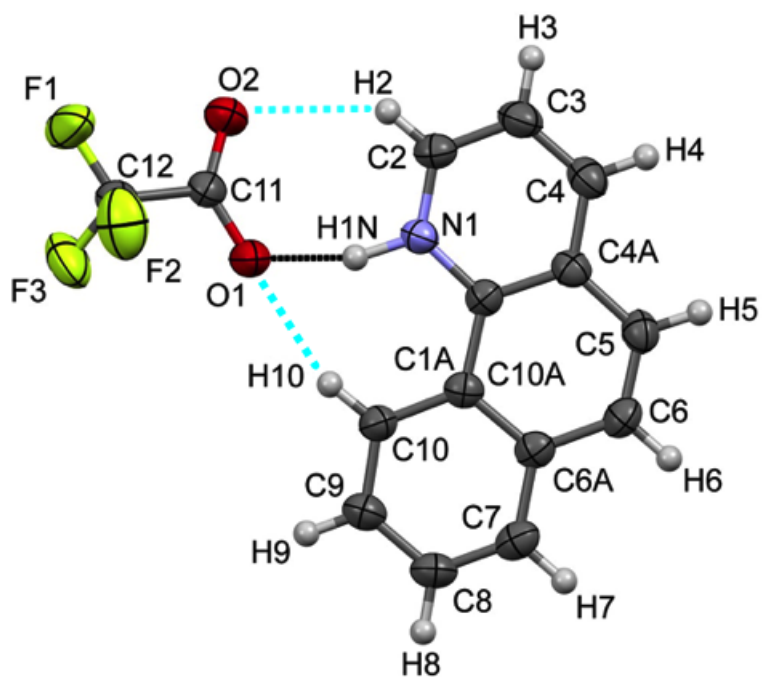
**Figure S32.** The individual disorder orientations in the X-ray structure of **8**. Displacement ellipsoids are drawn at the 50% probability level. The black-dotted lines are N-H...O/O-H...O hydrogen bonds and light blue-dotted lines represent weak intermolecular C-H...O interactions.



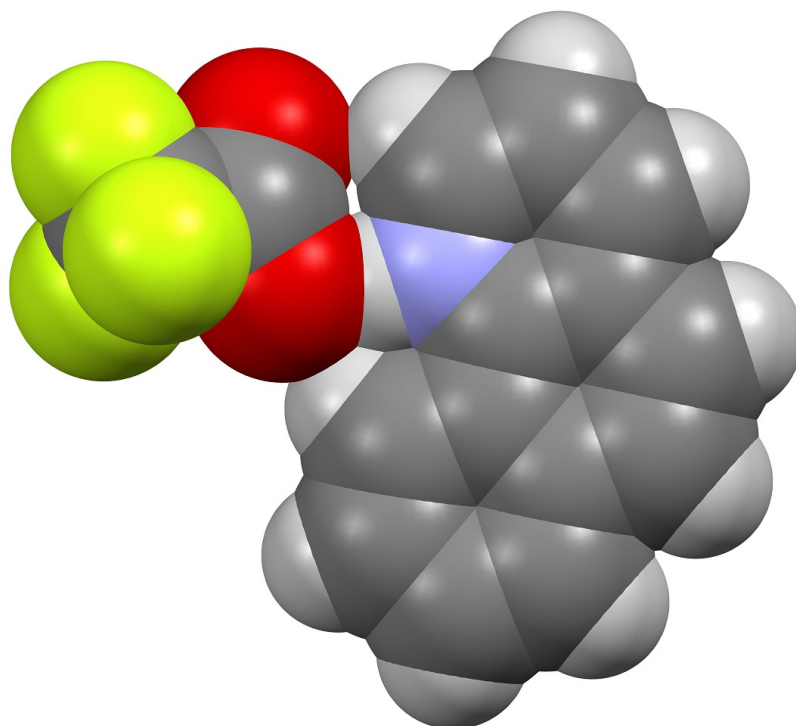
**Figure S33.** Displacement ellipsoid plot of **9**. Displacement ellipsoids are drawn at the 50% probability level. The black-dotted line represents N-H...O hydrogen bond.



**Figure S34.** Space-filling model of **9**.

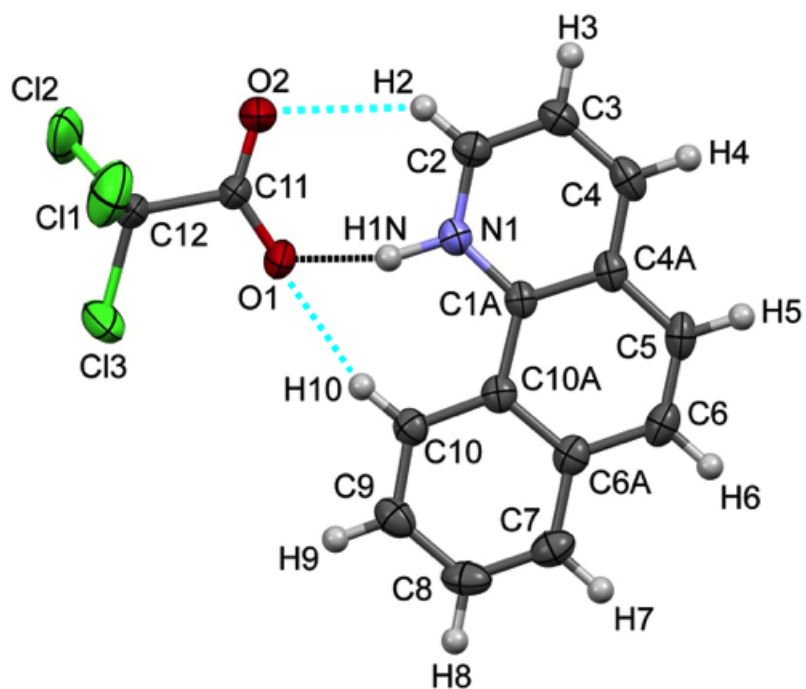


**Figure S35.** Displacement ellipsoid plot of **10**. Displacement ellipsoids are drawn at the 50% probability level. The black-dotted line is N-H...O hydrogen bond and light blue-dotted lines represent weak intermolecular C-H...O interactions.

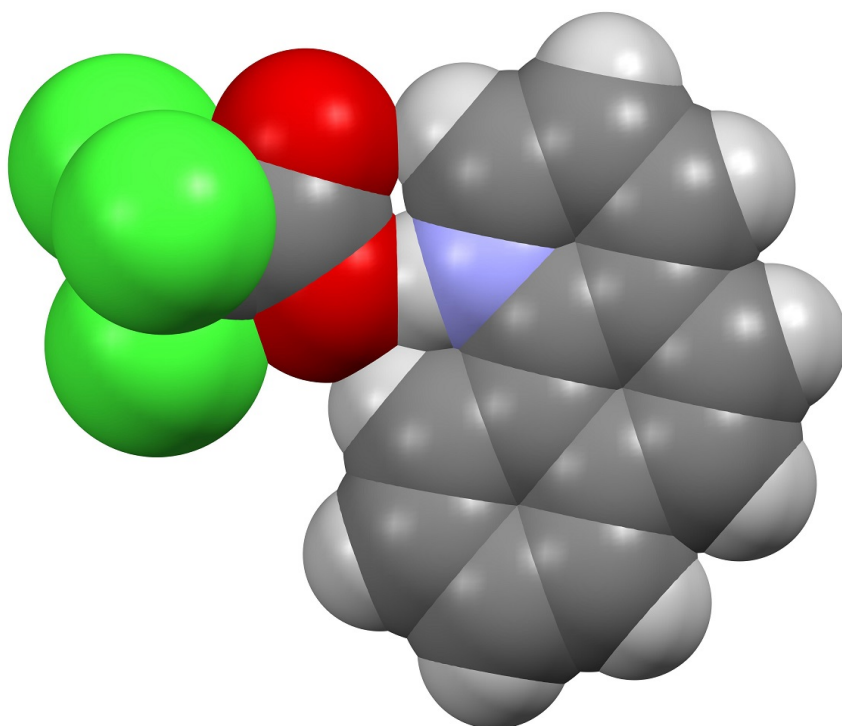


**Figure S36.** Space-filling model of **10**.

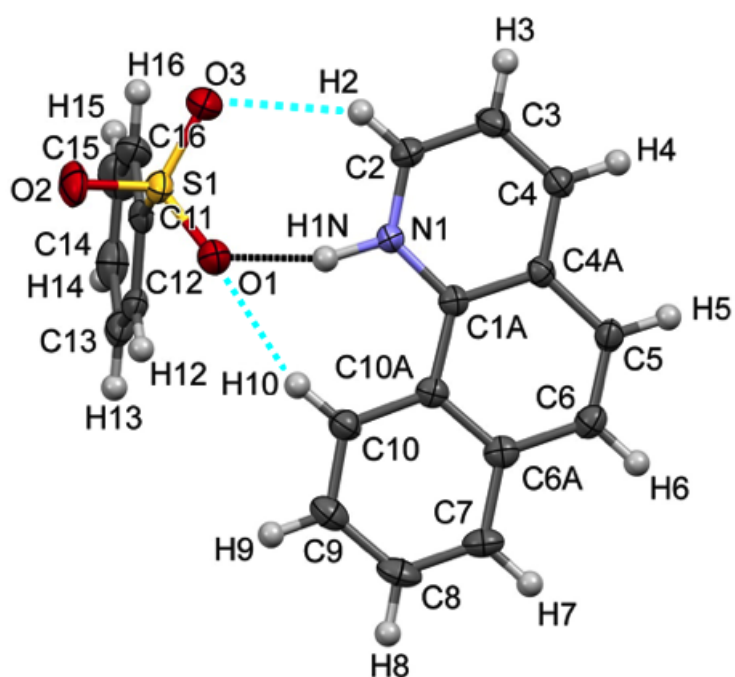




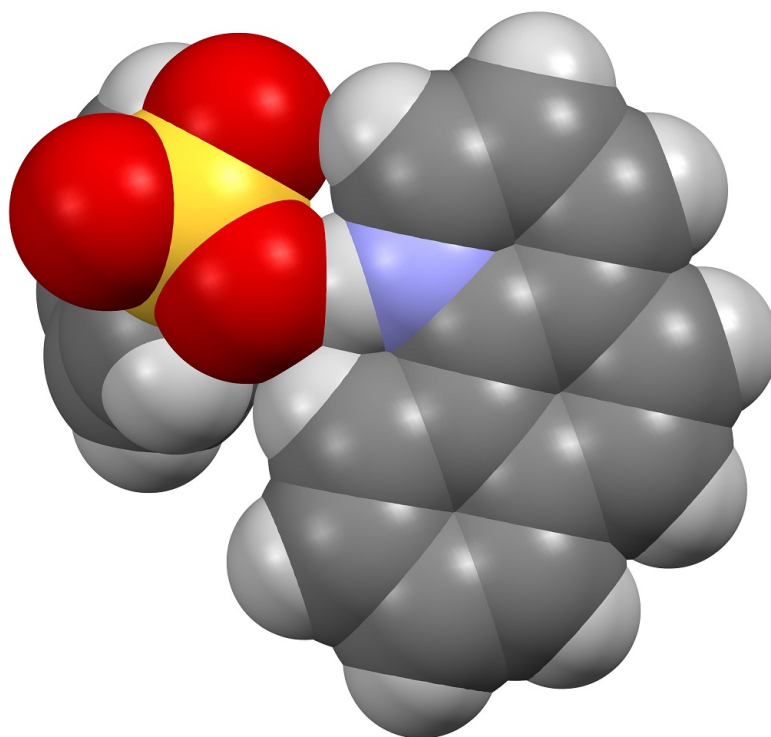
**Figure S37.** Displacement ellipsoid plot of **11**. Displacement ellipsoids are drawn at the 50% probability level. The black-dotted line is N–H···O hydrogen bond and light blue-dotted lines represent weak intermolecular C–H···O interactions.



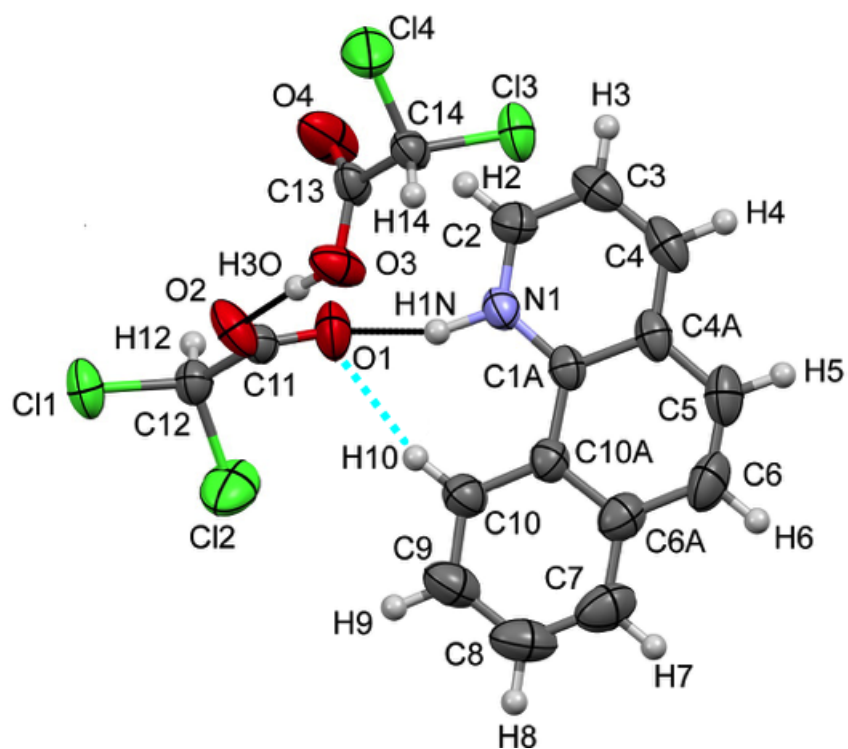
**Figure S38.** Space-filling model of **11**.



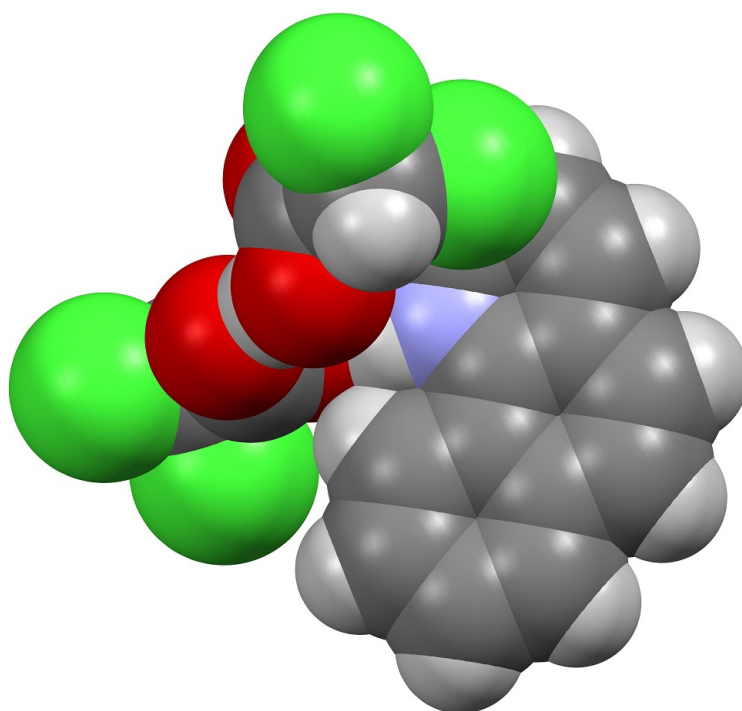
**Figure S39.** Displacement ellipsoid plot of **12**. Displacement ellipsoids are drawn at the 50% probability level. The black-dotted line is N–H $\cdots$ O hydrogen bond and light blue-dotted lines represent weak intermolecular C–H $\cdots$ O interactions.



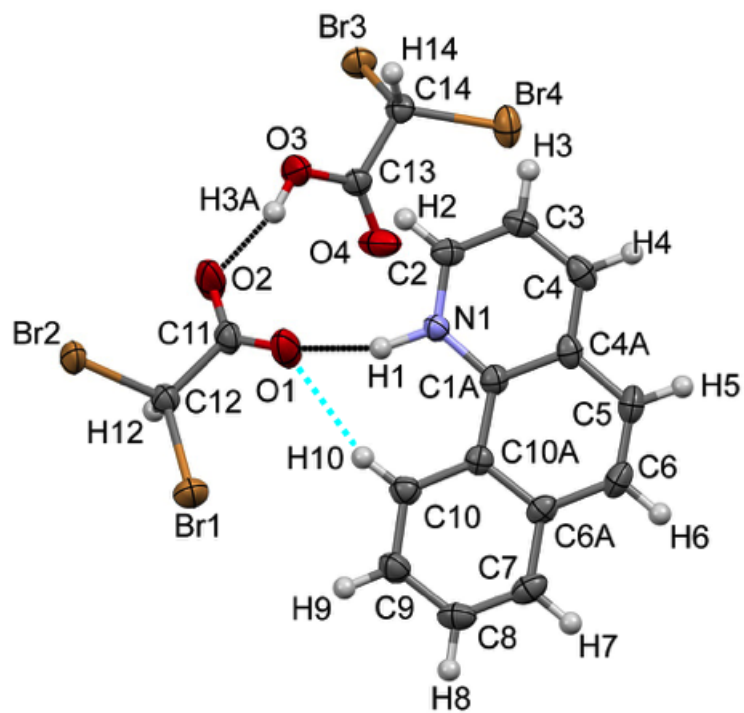
**Figure S40.** Space-filling model of **12**.



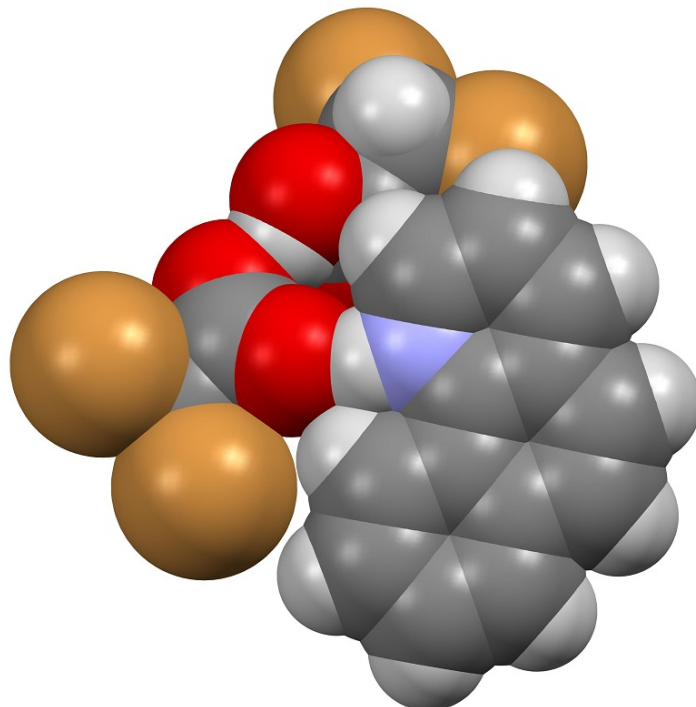
**Figure S41.** Displacement ellipsoid plot of **13**. Displacement ellipsoids are drawn at the 50% probability level. The black-dotted lines represent N-H...O/O-H...O hydrogen bonds and light blue-dotted line represents weak intermolecular C-H...O interaction.



**Figure S42.** Space-filling model of **13**.



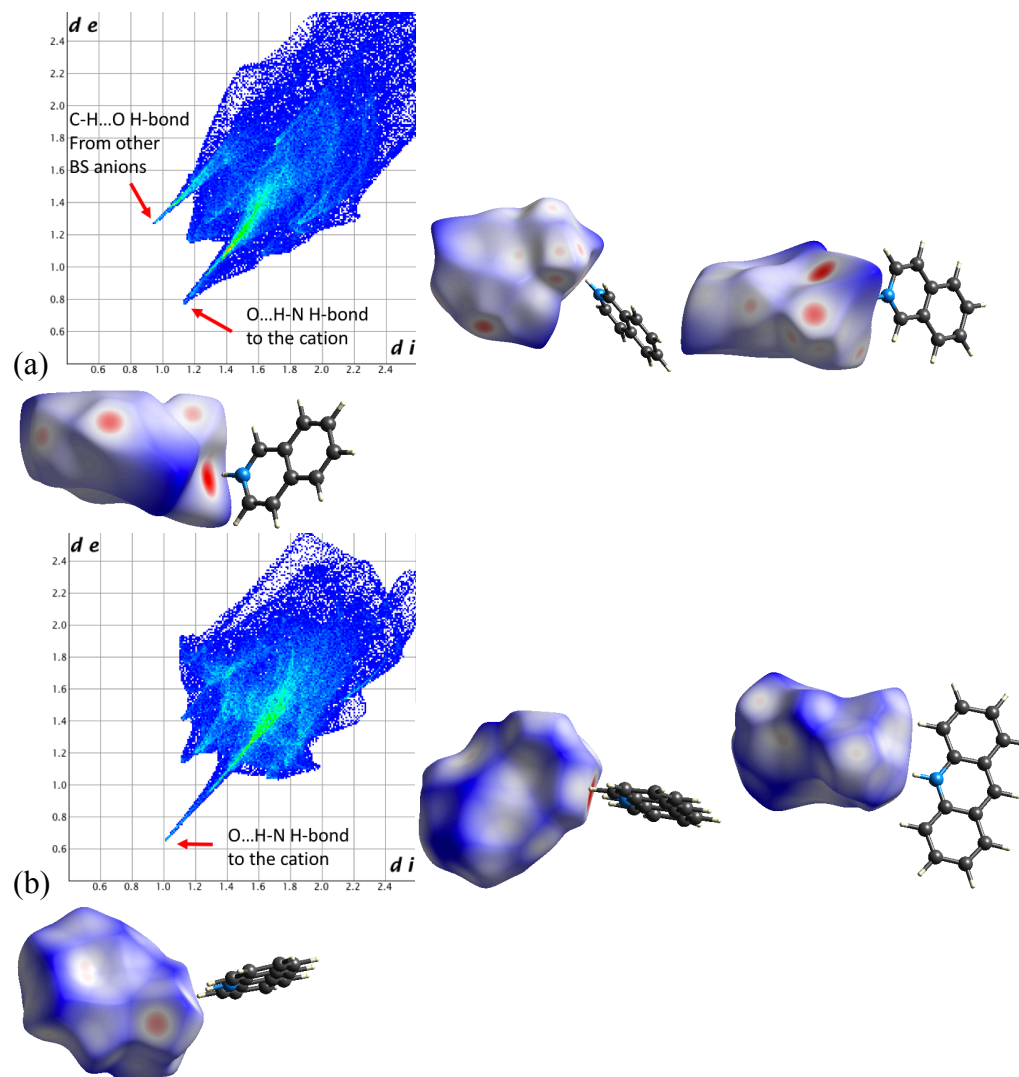
**Figure S43.** Displacement ellipsoid plot of **14**. Displacement ellipsoids are drawn at the 50% probability level. The black-dotted lines represent N–H...O/O–H...O hydrogen bonds and light blue-dotted line represents weak intermolecular C–H...O interaction.



**Figure S44.** Space-filling model of **14**.

## 4.2 Hirshfeld Surface Analysis for 3, 6 and 12

Hirshfeld surface plots and 2-D fingerprint calculations were made using Crystal Explorer package version 17.5. X-ray crystal structure files ("cifs") were imported, and Hirshfeld surfaces were generated for all base-acid complexes using very high resolution available in Crystal Explorer package version 17.5 and mapped with the  $d_{norm}$ . The corresponding contact distances to the Hirshfeld surfaces and fingerprint plots can be found in the following figures.



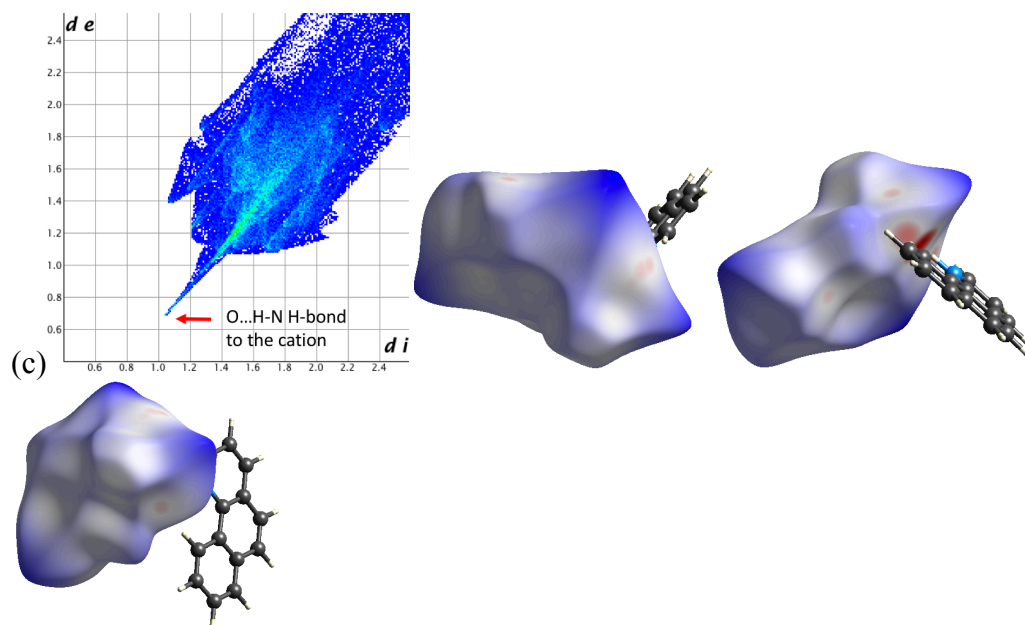


**Figure S45.** Full fingerprint regions of the benzene sulfonate (BS) anion in the compound (a) **3**, (b) **6**, and (c) **12**, and three views of the intermolecular contacts to the Hirshfeld surface of the BS anion. In the fingerprint plot  $d_i$  represents closest internal distance from a given point on the Hirshfeld surface, and  $d_e$  is the closest external contact [in Å].

## 5. Theoretical methods

For the calculations, we have used the M06-2X functional<sup>10</sup> combined with the def2-TZVP basis set<sup>11</sup> in a nonpolar solvation environment (C-PCM dielectric = 7.43) as implemented in the Spartan18 program.<sup>12</sup> For the analysis of the O···N distances the geometries have been fully optimized and they correspond to true minima.

### 5.1 DFT study

The starting point for the optimizations was the charge-assisted hydrogen-bonded anion-cation ion pair ( $\text{O}\cdots\text{H-N}^+$ ) present in the solid-state and confirmed by the X-ray structures. The calculated structures for all the benzenesulfonate salts **3**, **6** and **12**, as well the DCA, DBA and CA acridine based **7**, **8**, and **9** are shown in the Figures S45 and S46.

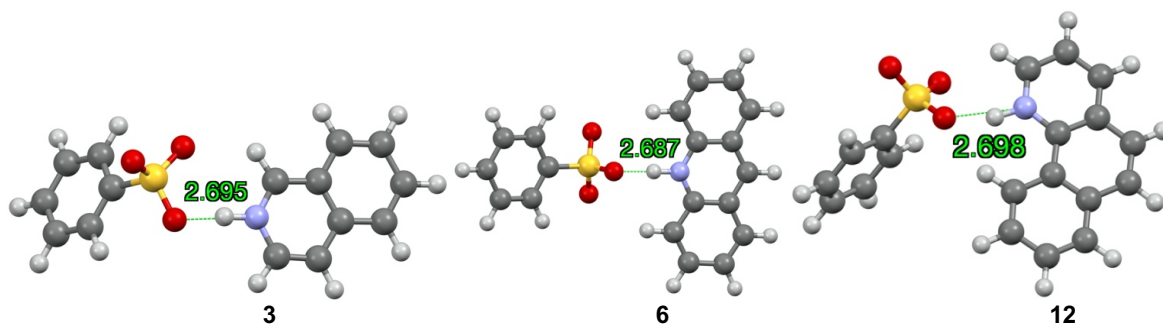


Figure S46. The calculated structures of **3**, **6** and **12** and their O···N distances (Å).

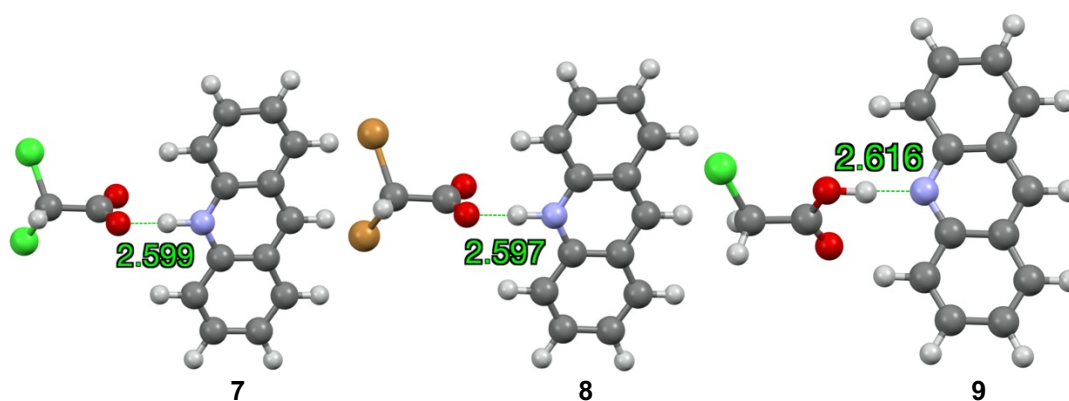


Figure S47. The calculated structures of **7**, **8** and **9** and their O···N distances (Å).

## References

- [1] B. Valeur, *Molecular Fluorescence: Principles and Applications*, Wiley-VCH Verlag GmbH, New York, p. 161, **2001**.
- [2] G. Grynkiewicz, M. Poenie, R. Tsien, *J. Biol. Chem.*, **1985**, *260*, 3440–3450.
- [3] R.W.W. Hooft, *COLLECT 1998*, Nonius BV, Delft, the Netherlands.
- [4] Otwinowski, Z.; Minor, W. *Methods in Enzymology, Macromolecular Crystallography, Part A* **1997**, *276*, 307-326. Edited by C. W. Carter Jr & R. M. Sweet, New York: Academic Press.
- [5] Sheldrick, G. M. *SADABS Version 2008/2* **1996**, University of Göttingen, Germany.
- [6] G. M. Sheldrick, *Acta Crystallogr. Sect. A*, **2015**, *71*, 3–8.
- [7] O. V Dolomanov, L. J. Bourhis, R. J. Gildea, J. A. K. Howard and H. Puschmann, *J. Appl. Crystallogr.*, **2009**, *42*, 339–341.
- [8] G. M. Sheldrick, *Acta Crystallogr. Sect. C*, **2015**, *71*, 3–8.
- [9] F. H. Allen and I. J. Bruno, *Acta Cryst.* **2010**, *B66*, 380–386.
- [10] Y. Zhao and D. G. Truhlar, *Theor. Chem. Acc.*, **2008**, *120*, 215-41.
- [11] F. Weigend and R. Ahlrichs, *Phys. Chem. Chem. Phys.*, **2005**, *7*, 3297-305.
- [12] SPARTAN18, Wavefunction Inc.: Irvine, CA, USA, **2018**.